

# Stress and Texture

# Strain

◆ Two types of stresses:

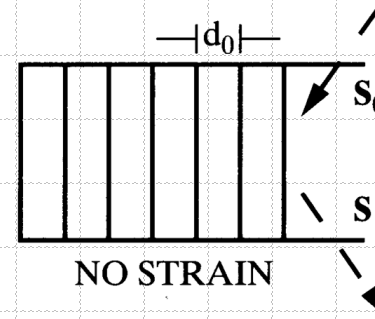
- microstresses – vary from one grain to another on a microscopic scale.
- macrostresses – stress is uniform over large distances.

◆ Usually:

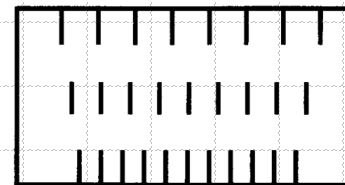
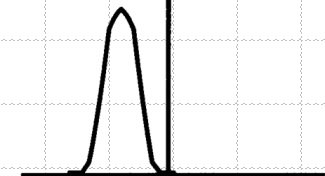
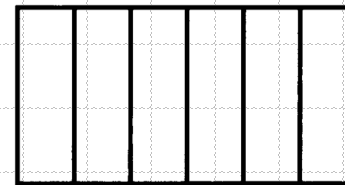
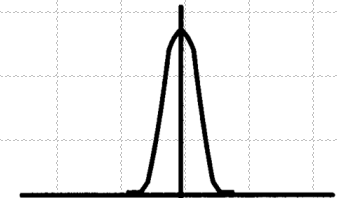
- macrostrain is uniform – produces peak shift
- microstrain is nonuniform – produces peak broadening

$$b = \Delta 2\theta = -2 \frac{\Delta d}{d} \tan \theta$$

CRYSTAL LATTICE



DIFFRACTION LINE

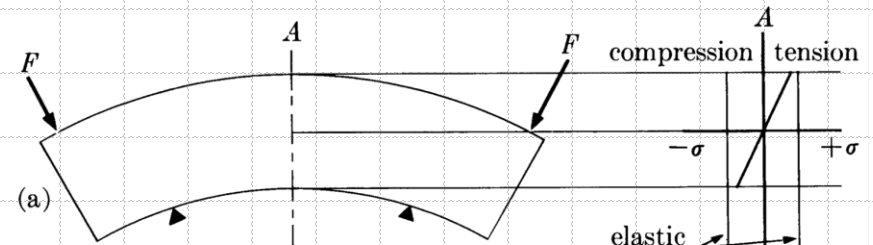


2θ

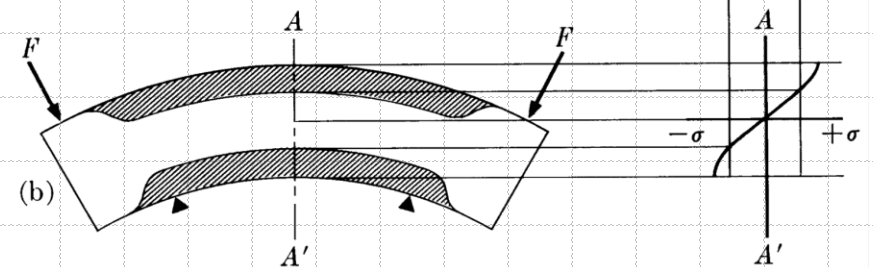
# Applied and Residual Stress

◆ Plastic flow can also set up residual stress.

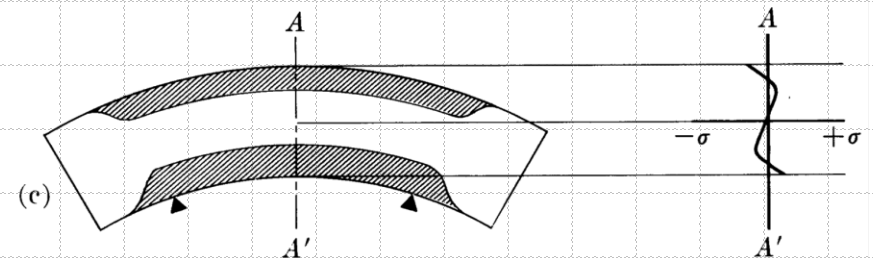
Loaded below elastic limit



Loaded beyond elastic limit



Unloaded



Shaded areas show regions plastically strained

# Methods to Measure Residual Stress

## ◆ X-ray diffraction.

- Nondestructive for the measurements near the surface:  $t < 2 \mu\text{m}$ .

## ◆ Neutron diffraction.

- Can be used to make measurements deeper in the material, but the minimum volume that can be examined is quite large (several  $\text{mm}^3$ ) due to the low intensity of most neutron beams.

## ◆ Dissection (mechanical relaxation).

- Destructive.

# General Principles

- ◆ Consider a rod of a cross-sectional area  $A$  stressed in tension by a force  $F$ .

Stress: 
$$\sigma_y = \frac{F}{A}, \quad \sigma_x, \sigma_z = 0$$

Stress  $\sigma_y$  produces strain  $\varepsilon_y$ :

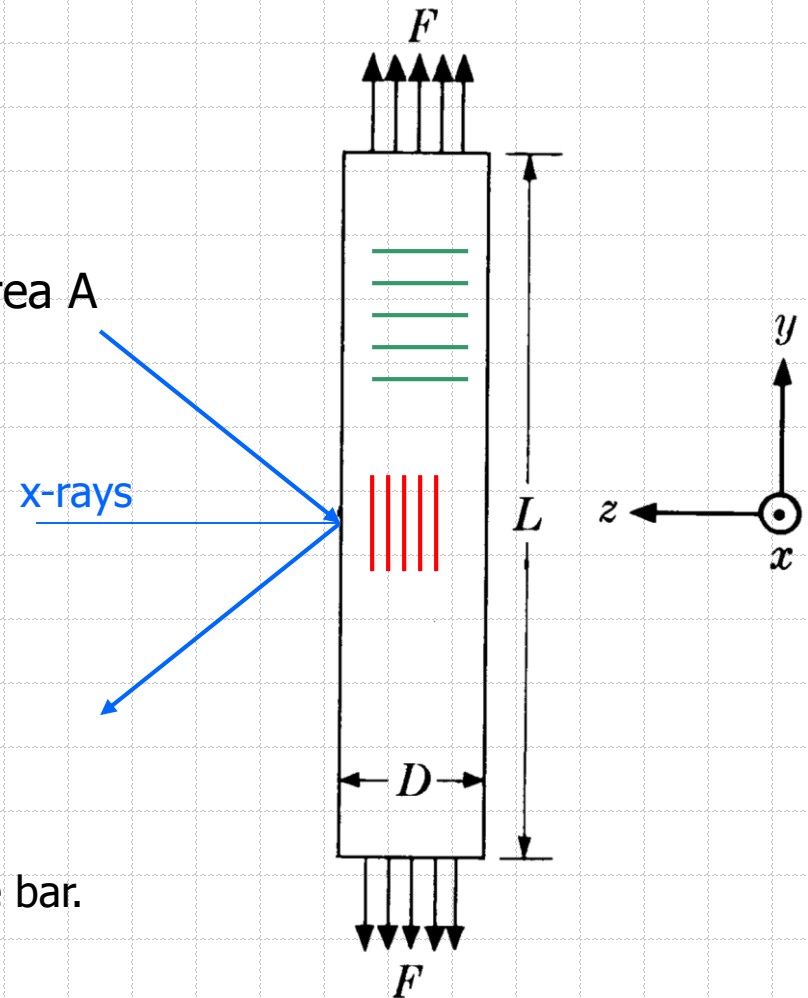
$$\varepsilon_y = \frac{\Delta L}{L} = \frac{L_f - L_0}{L_0}$$

$L_0$  and  $L_f$  are the original and final lengths of the bar.  
The strain is related to stress as:

$$\sigma_y = E\varepsilon_y$$

$L$  increases  $D$  decreases so:

$$\varepsilon_x = \varepsilon_z = \frac{\Delta D}{D} = \frac{D_f - D_0}{D_0}$$



$$\varepsilon_x = \varepsilon_z = -\nu\varepsilon_y \quad \text{for isotropic material}$$

$\nu$  – Poisson's ratio  
usually  $0.25 < \nu < 0.45$

# General Principles

- ◆ This provides measurement of the strain in the z direction since:

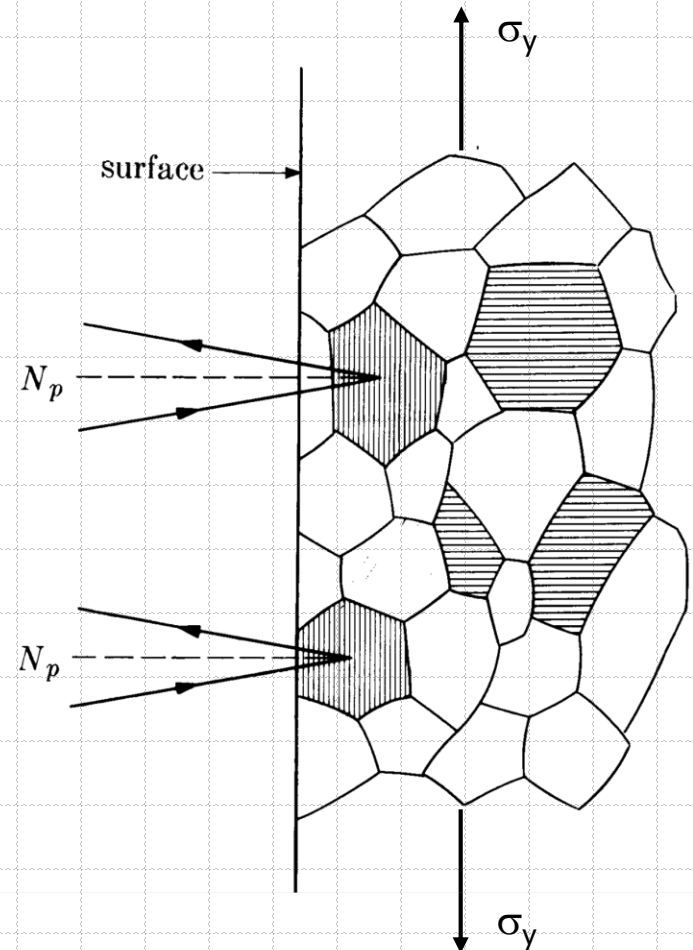
$$\varepsilon_z = \frac{d_n - d_0}{d_0}$$

Then the required stress will be:

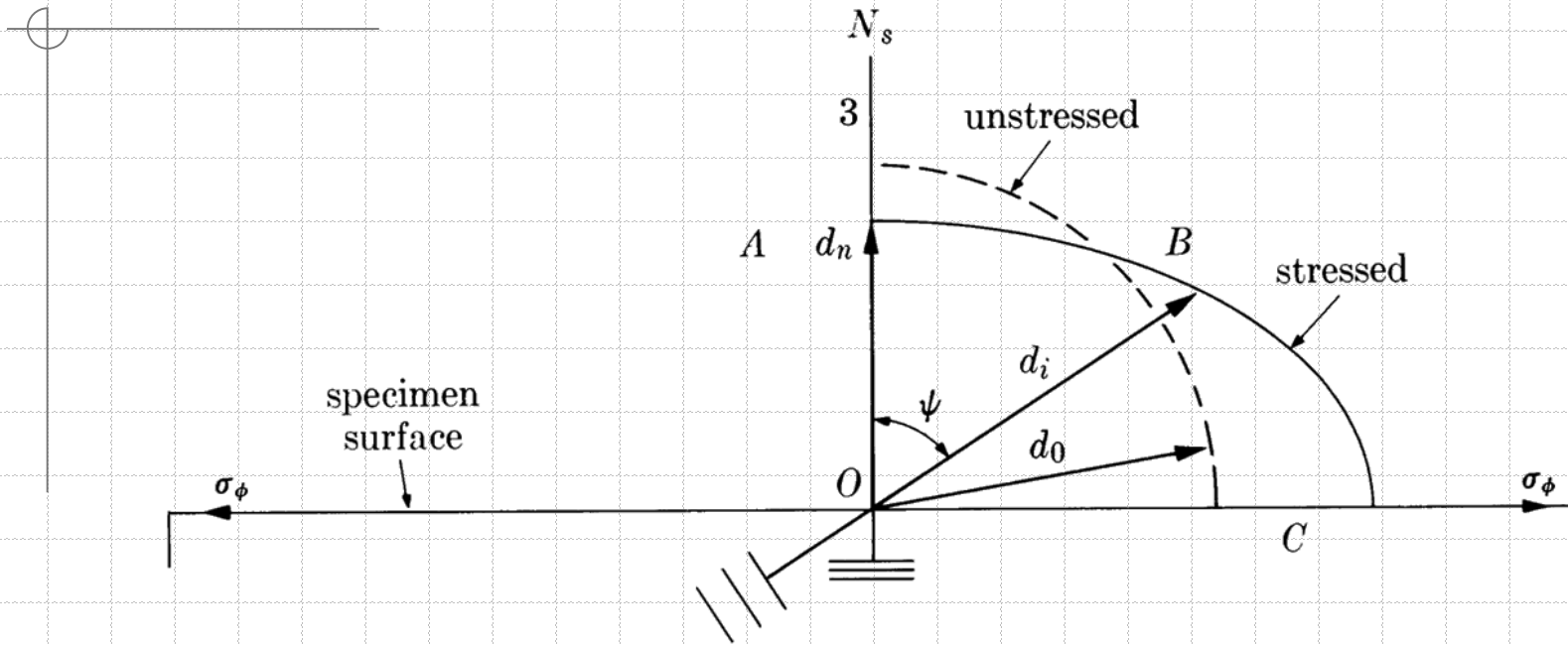
$$\sigma_y = -\frac{E}{\nu} \left( \frac{d_n - d_0}{d_0} \right)$$

## **Diffraction techniques do not measure stresses in materials directly**

- Changes in d-spacing are measured to give strain
- Changes in line width are measured to give microstrain
- The lattice planes of the individual grains in the material act as strain gauges



# General Principles



Vector diagram of plane spacings  $d$  for a tensile stress  $\sigma_\phi$

$$\sigma_y = -\frac{E}{\nu} \left( \frac{d_n - d_0}{d_0} \right)$$

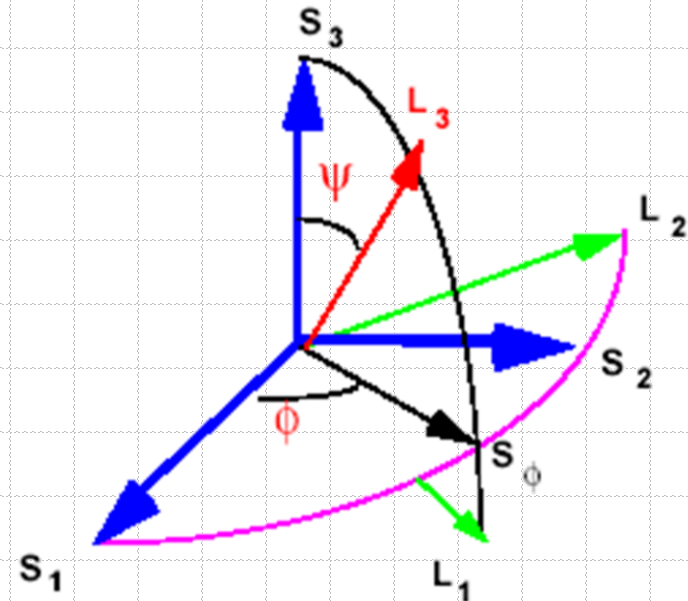
**we do not know  $d_0$  !**

# Elasticity

- ◆ In general there are stress components in two or three directions at right angles to one another, forming biaxial or triaxial stress systems.
  - Stresses in a material can be related to the set of three principal stresses  $\sigma_1$ ,  $\sigma_2$  and  $\sigma_3$ .
- ◆ To properly describe the results of a diffraction stress measurement we introduce a coordinate systems for the instrument and the sample. These two coordinate systems are related by two rotation angles  $\psi$  and  $\phi$ .

$L_i$  – laboratory coordinate system  
 $S_i$  – sample coordinate system

By convention the diffracting planes are normal to  $L_3$



# Elasticity

- ◆ In an anisotropic elastic material stress tensor  $\sigma_{ij}$  is related to the strain tensor  $\varepsilon_{kl}$  as:

$$\sigma_{ij} = C_{ijkl} \varepsilon_{kl}$$

where  $C_{ijkl}$  is elastic constants matrix.

Similarly:

$$\varepsilon_{ij} = S_{ijkl} \sigma_{kl}$$

where  $S_{ijkl}$  is elastic compliance matrix.

For isotropic compound:

$$\varepsilon_{ij} = \frac{1+\nu}{E} \sigma_{ij} - \delta_{ij} \frac{\nu}{E} \sigma_{kk}$$

where  $\delta_{ij}$  is Kronecker's delta, "kk" indicates the summation  $\sigma_{11} + \sigma_{22} + \sigma_{33}$

# Elasticity

◆ Or we can write it as:

$$\varepsilon_{11} = \frac{1}{E} [\sigma_{11} - \nu(\sigma_{22} + \sigma_{33})],$$

$$\varepsilon_{22} = \frac{1}{E} [\sigma_{22} - \nu(\sigma_{11} + \sigma_{33})],$$

$$\varepsilon_{33} = \frac{1}{E} [\sigma_{33} - \nu(\sigma_{11} + \sigma_{22})],$$

$$\varepsilon_{23} = \frac{1}{2\mu} \sigma_{23},$$

$$\varepsilon_{31} = \frac{1}{2\mu} \sigma_{31},$$

$$\varepsilon_{12} = \frac{1}{2\mu} \sigma_{12}$$

where

$$\mu = \frac{E}{2(1+\nu)}$$

shear modulus

# Elasticity

- ◆ Lets relate  $\varepsilon_{mn}$  in one coordinate system to that in another system through transformation matrix:

$$\varepsilon_{mn}^L = M_{mi}^{SL} M_{nj}^{SL} \varepsilon_{ij}^S$$

The transformation matrix is:

$$M^{SL} = \begin{bmatrix} \cos \phi \cos \psi & -\sin \phi & \cos \phi \sin \psi \\ \sin \phi \cos \psi & \cos \phi & \sin \phi \sin \psi \\ -\sin \psi & 0 & \cos \psi \end{bmatrix}$$

so that we find

$$\begin{aligned} \left( \varepsilon_{33}^L \right)_{\phi\psi} &= M_{3i}^{SL} M_{3j}^{SL} \varepsilon_{ij}^S \\ &= \varepsilon_{11}^S \cos^2 \phi \sin^2 \psi + \varepsilon_{12}^S \sin 2\phi \sin^2 \psi \\ &\quad + \varepsilon_{22}^S \sin^2 \phi \sin^2 \psi + \varepsilon_{33}^S \cos^2 \psi \\ &\quad + \varepsilon_{13}^S \cos \phi \sin 2\psi + \varepsilon_{23}^S \sin \phi \sin 2\psi \end{aligned}$$

# Elasticity

◆ In terms of stresses:

$$\begin{aligned} \left(\varepsilon_{33}^L\right)_{\phi\psi} &= \frac{1+\nu}{E} \left\{ \sigma_{11}^S \cos^2 \phi + \sigma_{12}^S \sin 2\phi + \sigma_{22}^S \sin^2 \phi - \sigma_{33}^S \right\} \sin^2 \psi + \frac{1+\nu}{E} \sigma_{33}^S \\ &\quad - \frac{\nu}{E} \left( \sigma_{11}^S + \sigma_{22}^S + \sigma_{33}^S \right) + \frac{1+\nu}{E} \left\{ \sigma_{13}^S \cos \phi + \sigma_{23}^S \sin \phi \right\} \sin 2\psi \\ &= \frac{d_{\phi\psi} - d_0}{d_0} \end{aligned}$$

# Biaxial and Triaxial Stress Analysis

◆ Biaxial stress tensor is in the form:

$$\begin{bmatrix} \sigma_{11} & 0 & 0 \\ 0 & \sigma_{22} & 0 \\ 0 & 0 & 0 \end{bmatrix}$$

since stress normal to a free surface must be zero:  $\sigma_{ij} \mathbf{n}_j = 0$

For our tensor lets define:

$$\sigma_{\phi}^S = \sigma_{11}^S \cos^2 \phi + \sigma_{22}^S \sin^2 \phi$$

Then the equation for strain becomes:

$$\varepsilon_{\psi\phi}^L = \frac{d_{\phi\psi} - d_0}{d_0} = \frac{1+\nu}{E} \sigma_{\phi}^S \sin^2 \psi - \frac{\nu}{E} (\sigma_{11}^S + \sigma_{22}^S)$$

# The $\sin^2\psi$ Method

- ◆ Stress  $\sigma_{33}$  is zero, but strain  $\varepsilon_{33}$  is not zero. It has finite value given by the Poisson contractions due to  $\sigma_{11}$  and  $\sigma_{22}$ :

$$\varepsilon_{33}^S = -\nu(\varepsilon_{11}^S + \varepsilon_{22}^S) = -\frac{\nu}{E}(\sigma_{11}^S + \sigma_{22}^S)$$

Then strain equation can be written as:

$$\varepsilon_{\phi\psi}^L - \varepsilon_{33}^S = \frac{(1+\nu)\sigma_{\phi}^S}{E} \sin^2 \psi$$

$$\begin{aligned} \varepsilon_{\phi\psi}^L - \varepsilon_{33}^S &= \frac{d_{\phi\psi} - d_0}{d_0} - \frac{d_n - d_0}{d_0} \\ &= \frac{d_{\phi\psi} - d_n}{d_0} = \frac{(1+\nu)\sigma_{\phi}^S}{E} \sin^2 \psi \end{aligned}$$

# The $\sin^2\psi$ Method

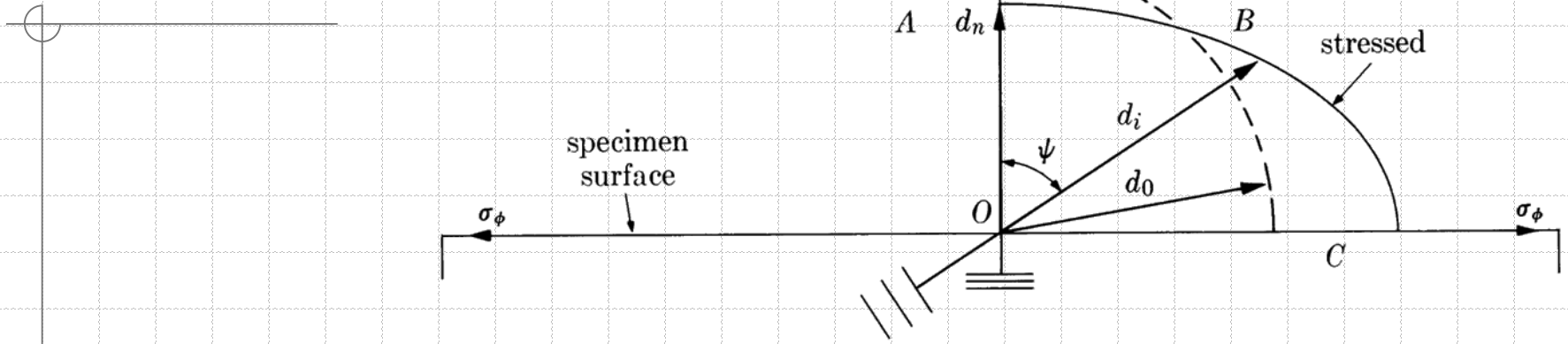
- ◆ We make ingenious approximation (by Glocker *et al.* in 1936):
  - $d_n$ ,  $d_i$  and  $d_0$  are very nearly equal to one another,
  - $(d_i - d_n)$  is small compared to  $d_0$ ,
  - unknown  $d_0$  is replaced by  $d_i$  or  $d_n$  with negligible error.

$$\frac{d_{\phi\psi} - d_n}{d_n} = \frac{(1 + \nu)\sigma_\phi}{E} \sin^2 \psi$$

$$\sigma_\phi = \frac{E}{(1 + \nu)\sin^2 \psi} \left( \frac{d_{\phi\psi} - d_n}{d_n} \right)$$

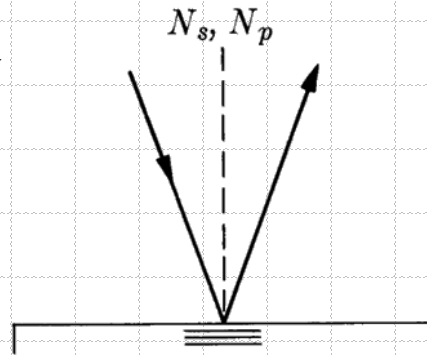
- The stress in a surface can be determined by measuring the  $d$ -spacing as a function of the angle  $\psi$  between the surface normal and the diffracting plane normal
- Measurements are made in the back-reflection regime ( $2\theta \rightarrow 180^\circ$ ) to obtain maximum accuracy

# The $\sin^2\psi$ Method

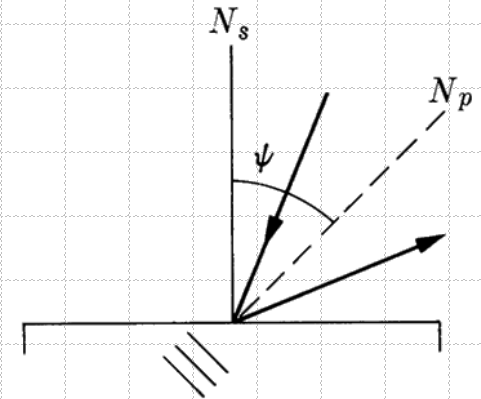


Vector diagram of plane spacings  $d$  for a tensile stress  $\sigma_\phi$

$$\frac{d_{\phi\psi} - d_n}{d_n} = \frac{(1+\nu)\sigma_\phi}{E} \sin^2\psi$$



Measurement of  $d_n$



Measurement of  $d_i$

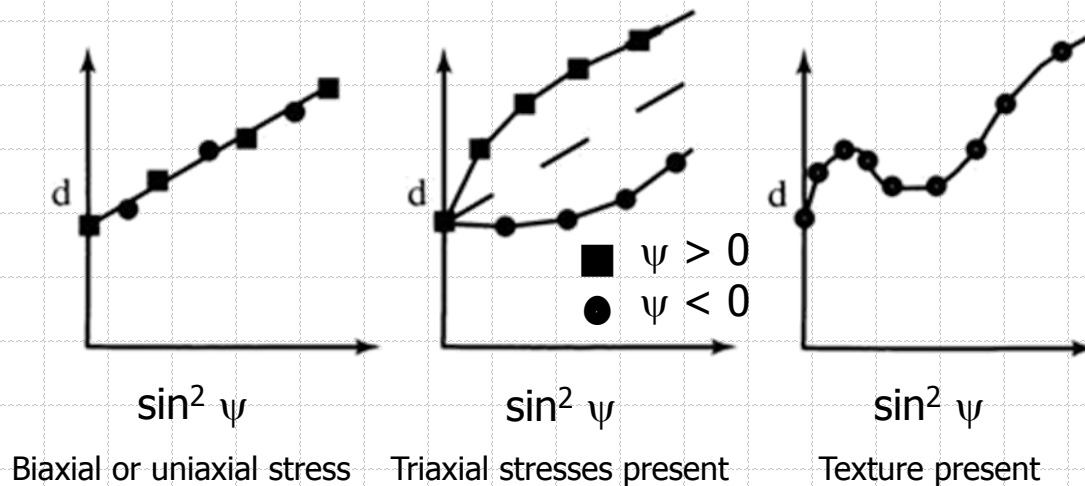
# The $\sin^2\psi$ Method

- ◆ Lets assume that stresses in zx plane are equal. This is referred to as an equal-biaxial stress state. We can write sample frame stress as:

$$\begin{bmatrix} \sigma & 0 & 0 \\ 0 & \sigma & 0 \\ 0 & 0 & 0 \end{bmatrix}$$

No stress dependence on  $\phi$

$$\frac{d_\psi - d_n}{d_n} = \frac{(1+\nu)\sigma}{E} \sin^2 \psi$$



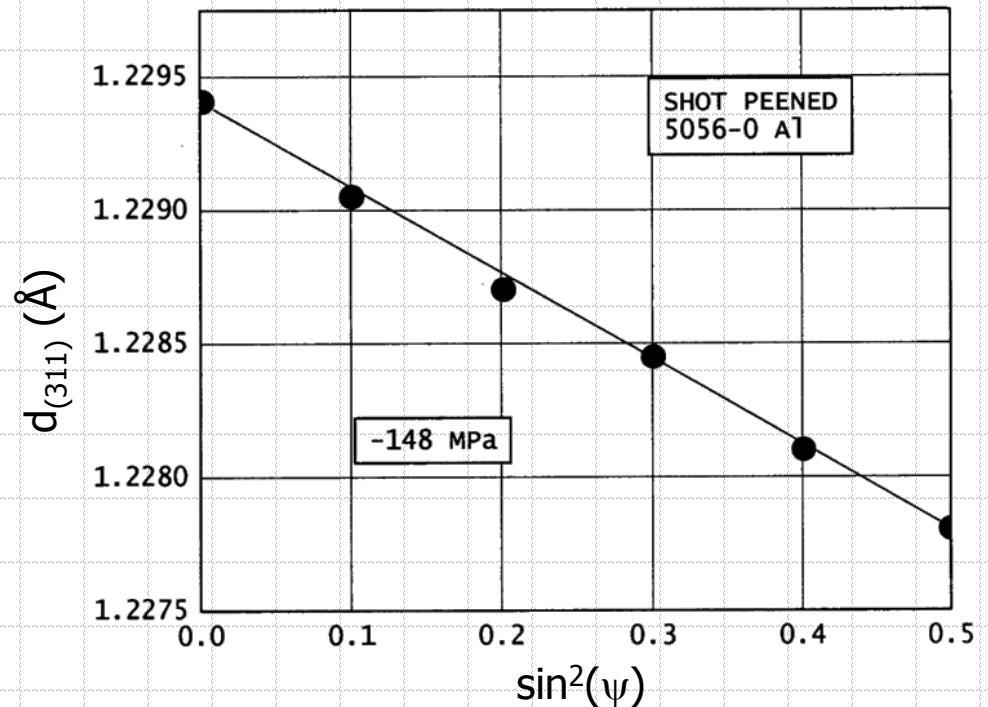
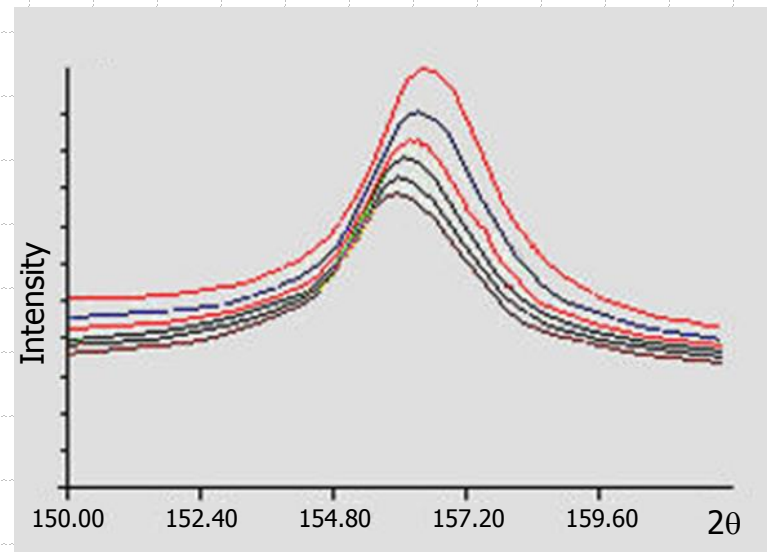
# The $\sin^2\psi$ Method

$$d_\psi = \frac{(1+\nu)\sigma}{E} d_n \sin^2 \psi + d_n$$

Slope of the plot is:

$$\frac{\partial d_\psi}{\partial \sin^2 \psi} = \frac{(1+\nu)}{E} \sigma d_n$$

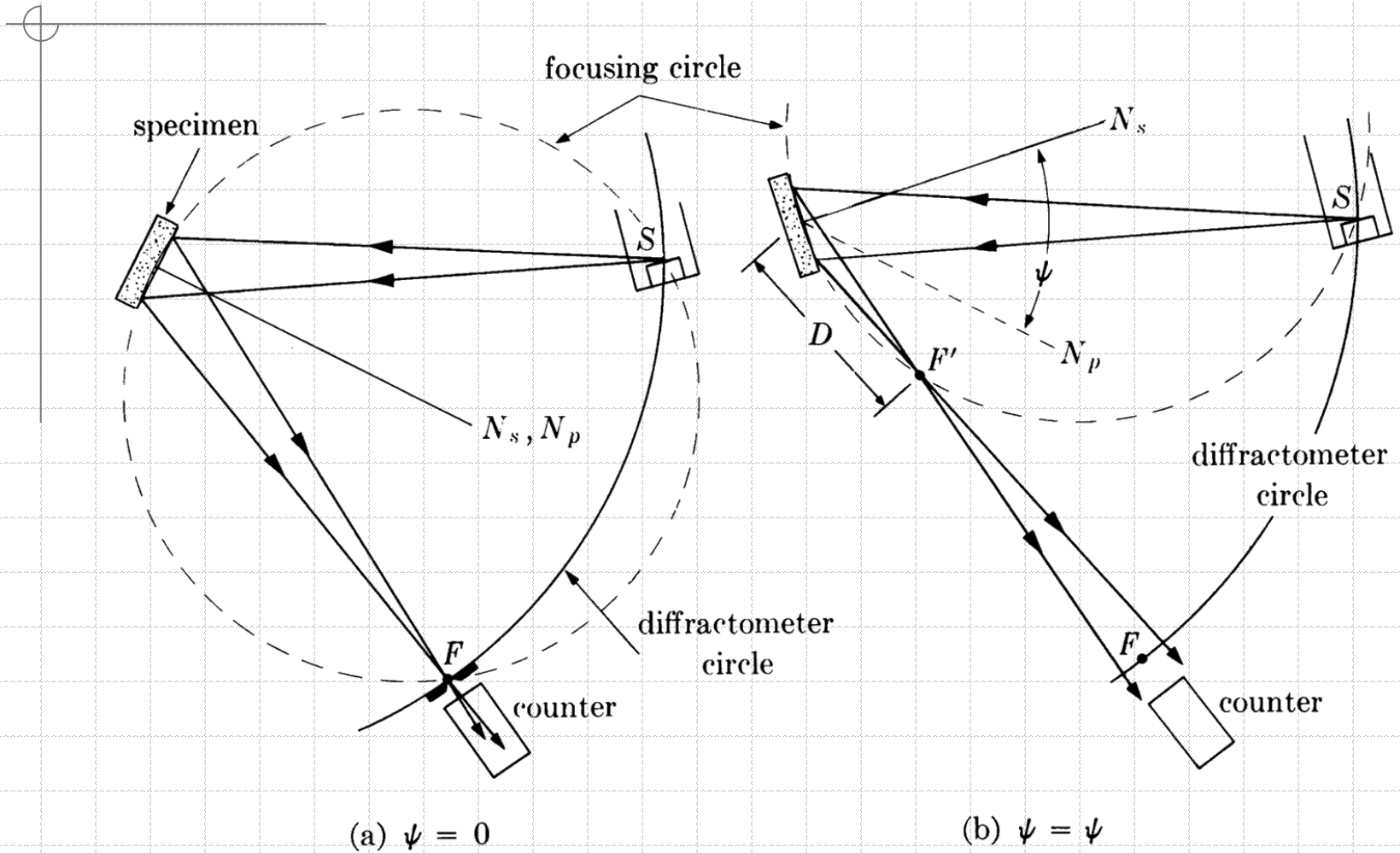
Generally  $\nu$  and  $E$  are well-known constants



Linear dependence of  $d_{(311)}$  upon  $\sin^2\psi$  for shot peened 5056-0 aluminum.

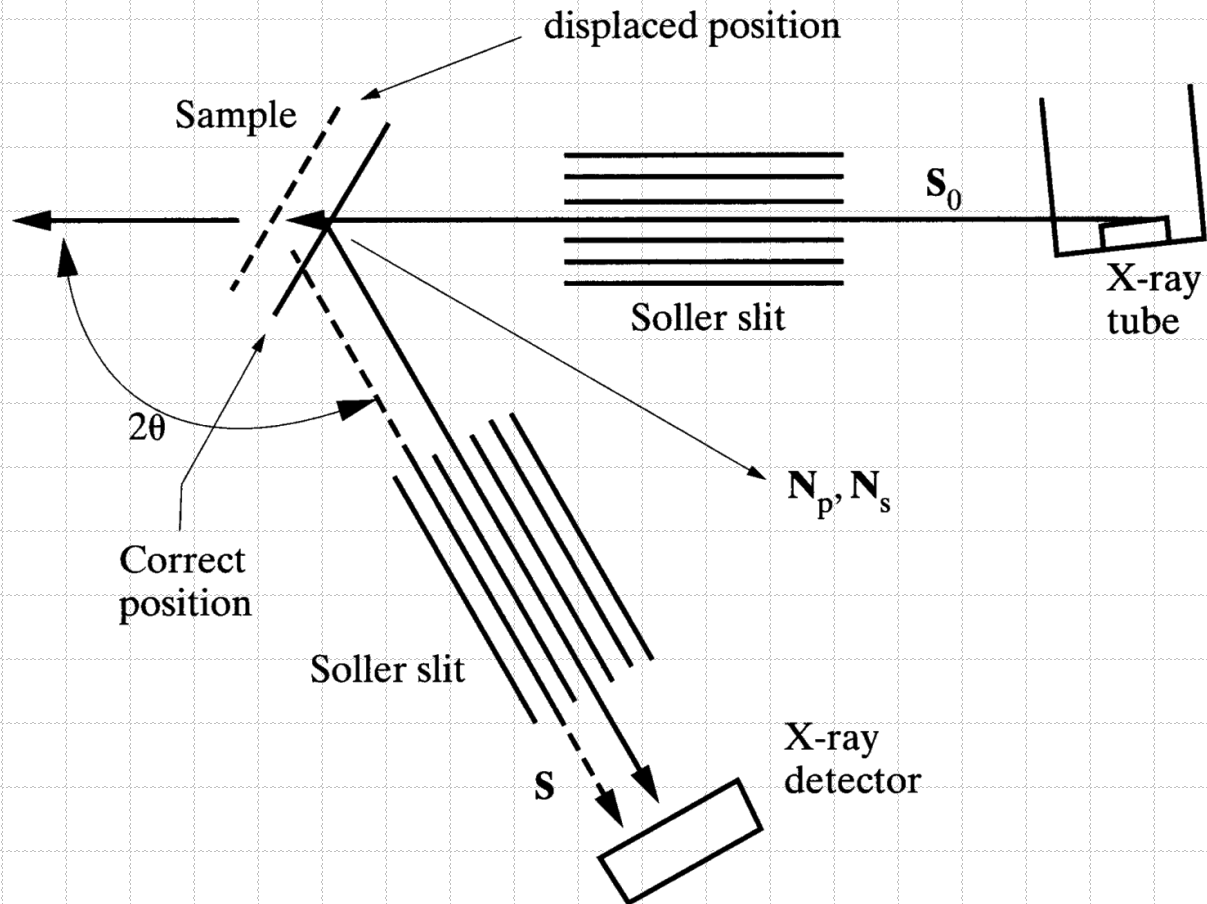
# Diffractometer Method

$$\frac{D}{R} = \frac{\sin(\theta - \psi)}{\sin(\theta + \psi)}$$



# Diffractometer Method

- ◆ The effect of sample or  $\psi$ -axis displacement can be minimized if a parallel beam geometry is used instead of focused beam geometry.



# Measurement of Line Position

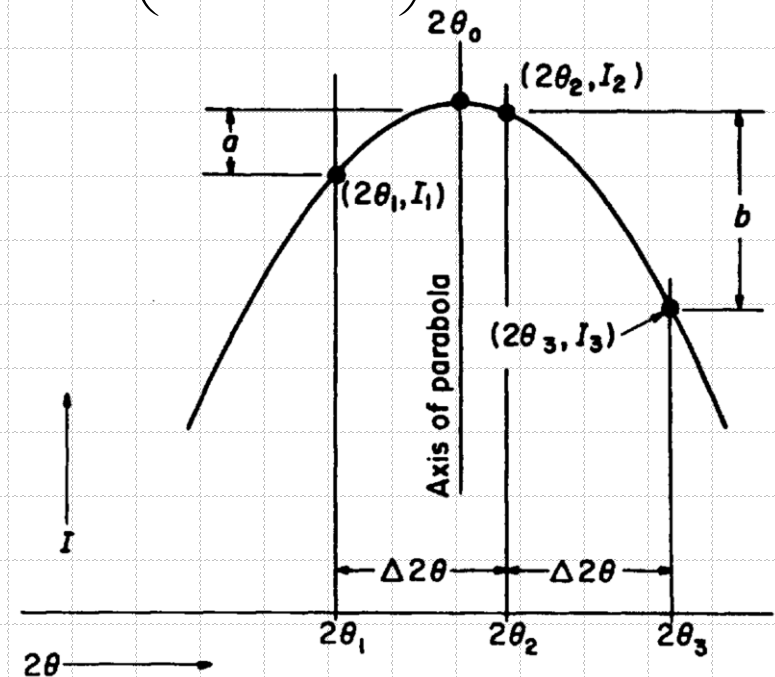
- ◆ Sample must remain on the diffractometer axis as  $\psi$  is changed (even if the sample is large)
- ◆ Radial motion of the detector to achieve focussing must not change the measured  $2\theta$
- ◆ L-P factor may vary significantly across a (broad) peak  $\Rightarrow LPA = \left( \frac{1 + \cos^2 2\theta}{\sin^2 \theta} \right) (1 - \tan \psi \cot \theta)$
- ◆ Absorption will vary when  $\Psi \neq 0$
- ◆ Measurement of peak position often requires fitting the peak with a parabola:

$$2\theta_0 = 2\theta_1 + \frac{\Delta 2\theta}{2} \left( \frac{3a + b}{a + b} \right)$$

$$a = I_2 - I_1$$

$$b = I_2 - I_3$$

$$\Delta 2\theta = 2\theta_2 - 2\theta_1 = 2\theta_3 - 2\theta_2$$



# Measurements of Stress in Thin Films

- ◆ Thin films are usually textured. No difficulty with moderate degree of preferred orientation.
- ◆ Sharp texture has the following effects:
  - Diffraction line strong at  $\psi = 0$  and absent at  $\psi = 45^\circ$ .
  - If material anisotropic E will depend on direction in the specimen. Oscillations of  $d$  vs  $\sin^2\psi$ .

# Measurements of Stress in Thin Films

◆ In thin films we have a biaxial stress, so:

$$\frac{d_{\phi\psi} - d_n}{d_n} = \frac{(1+\nu)\sigma_\phi}{E} \sin^2 \psi$$

If we have equal-biaxial stress then it is even simpler:

$$\frac{a_\psi - a_n}{a_n} = \frac{d_{hkl}^\psi - d_{hkl}^n}{d_{hkl}^n} = \frac{(1+\nu)\sigma}{E} \sin^2 \psi$$

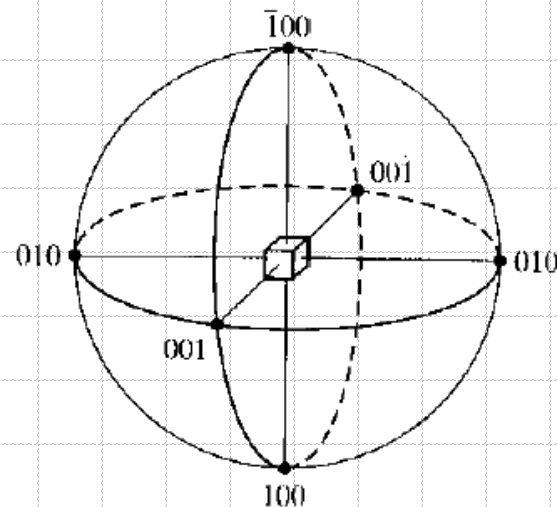
We can calculate  $\psi$  for any unit cell and any orientation. For cubic:

$$\psi = a \cos \left( \frac{h_\perp h + k_\perp k + l_\perp l}{\sqrt{(h_\perp^2 + k_\perp^2 + l_\perp^2)(h^2 + k^2 + l^2)}} \right)$$

Symbols  $h_\perp$ ,  $k_\perp$  and  $l_\perp$  define (hkl) - oriented film

# Texture Analysis

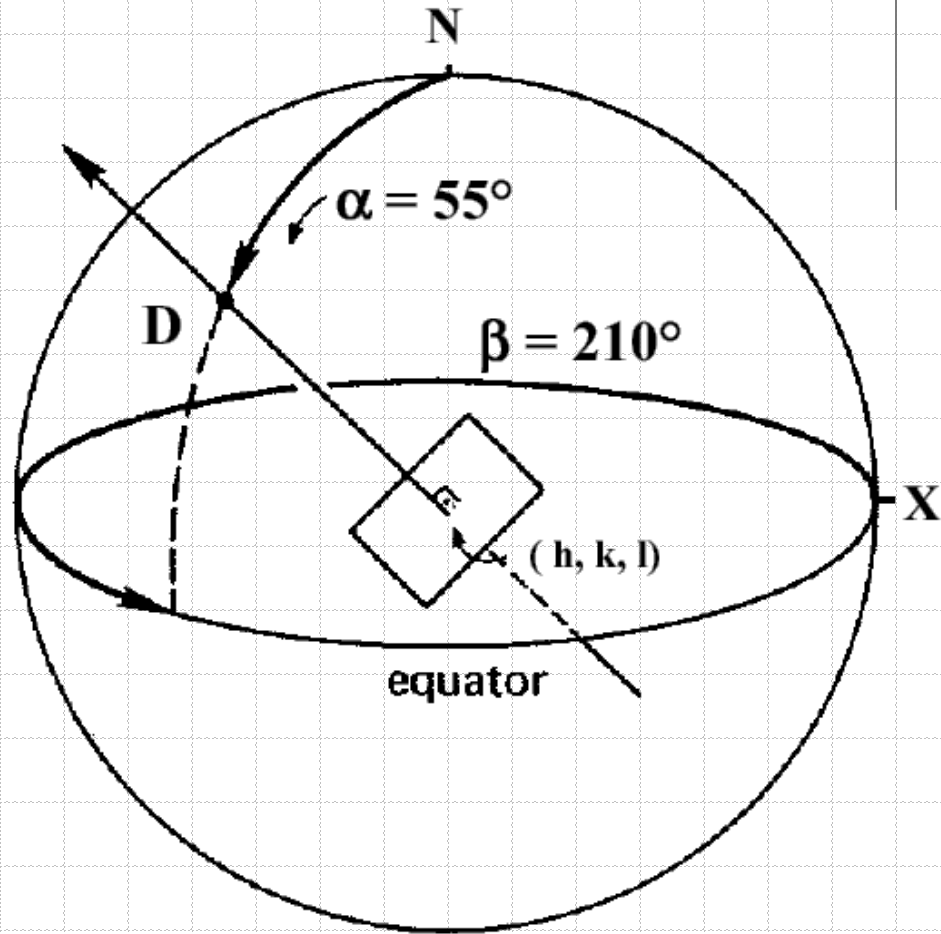
- ◆ The determination of the lattice preferred orientation of the crystallites in a polycrystalline aggregate is referred to as texture analysis.
- ◆ The term texture is used as a broad synonym for preferred crystallographic orientation in a polycrystalline material, normally a single phase.
- ◆ The preferred orientation is usually described in terms of pole figures.



{100} poles of a cubic crystal

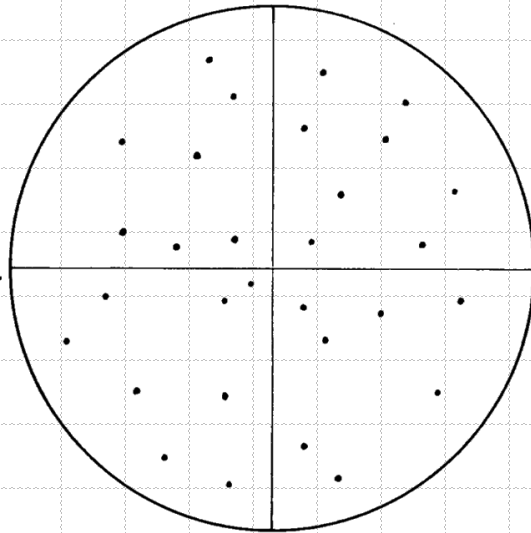
# The Pole Figures

- ◆ Let us consider the plane  $(h\ k\ l)$  in a given crystallite in a sample. The direction of the plane normal is projected onto the sphere around the crystallite.
- ◆ The point where the plane normal intersects the sphere is defined by two angles: pole distance  $\alpha$  and an azimuth  $\beta$ .
- ◆ The azimuth angle is measured counter clock wise from the point X.

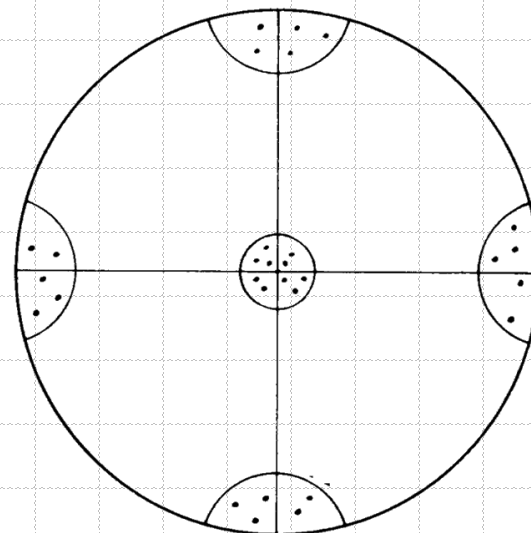


# The Pole Figures

- ◆ Let us now assume that we project the plane normals for the plane (h k l) from all the crystallites irradiated in the sample onto the sphere.
- ◆ Each plane normal intercepting the sphere represents a point on the sphere. These points in return represent the Poles for the planes (h k l) in the crystallites. The number of points per unit area of the sphere represents the pole density.



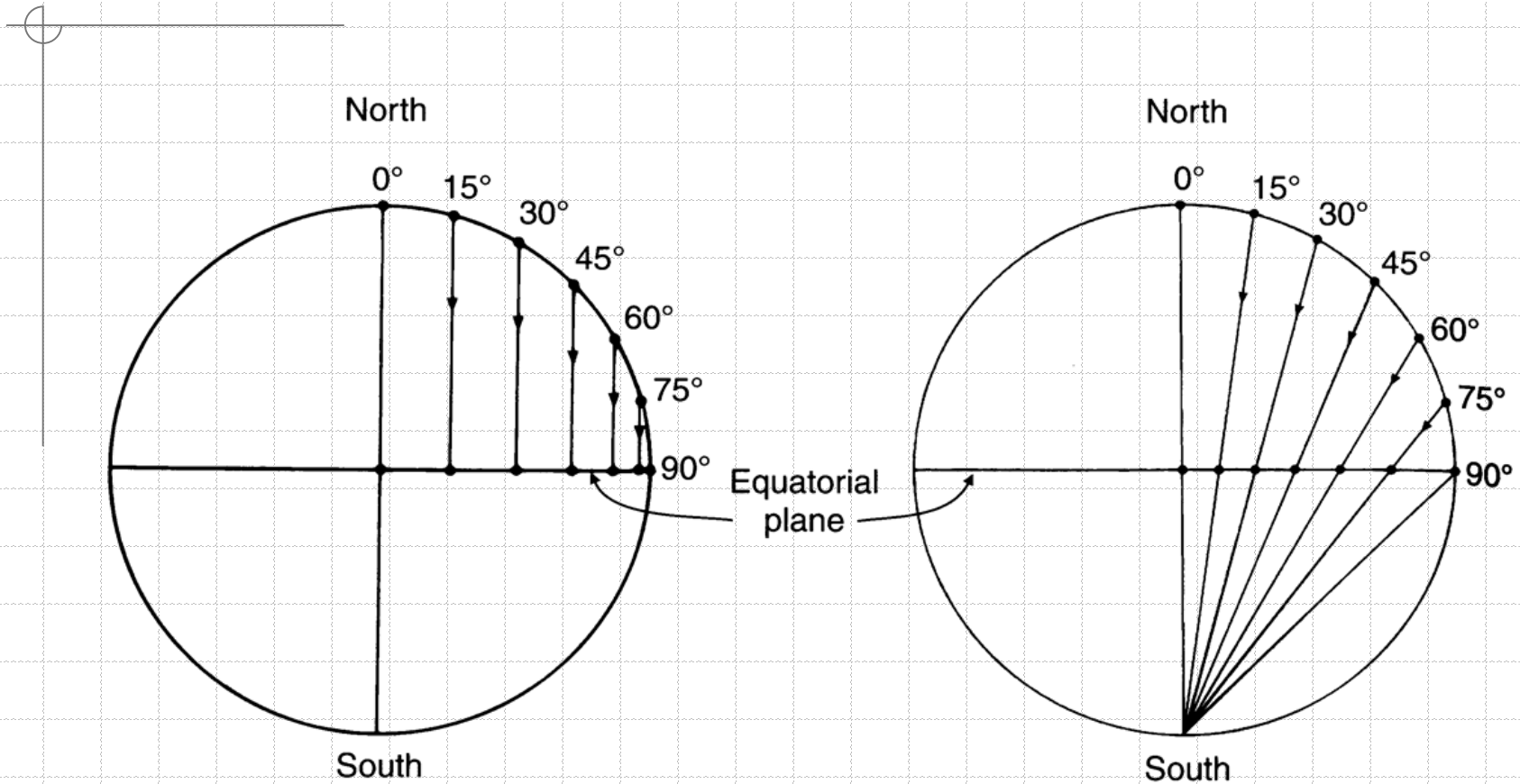
Random orientation



Preferred orientation



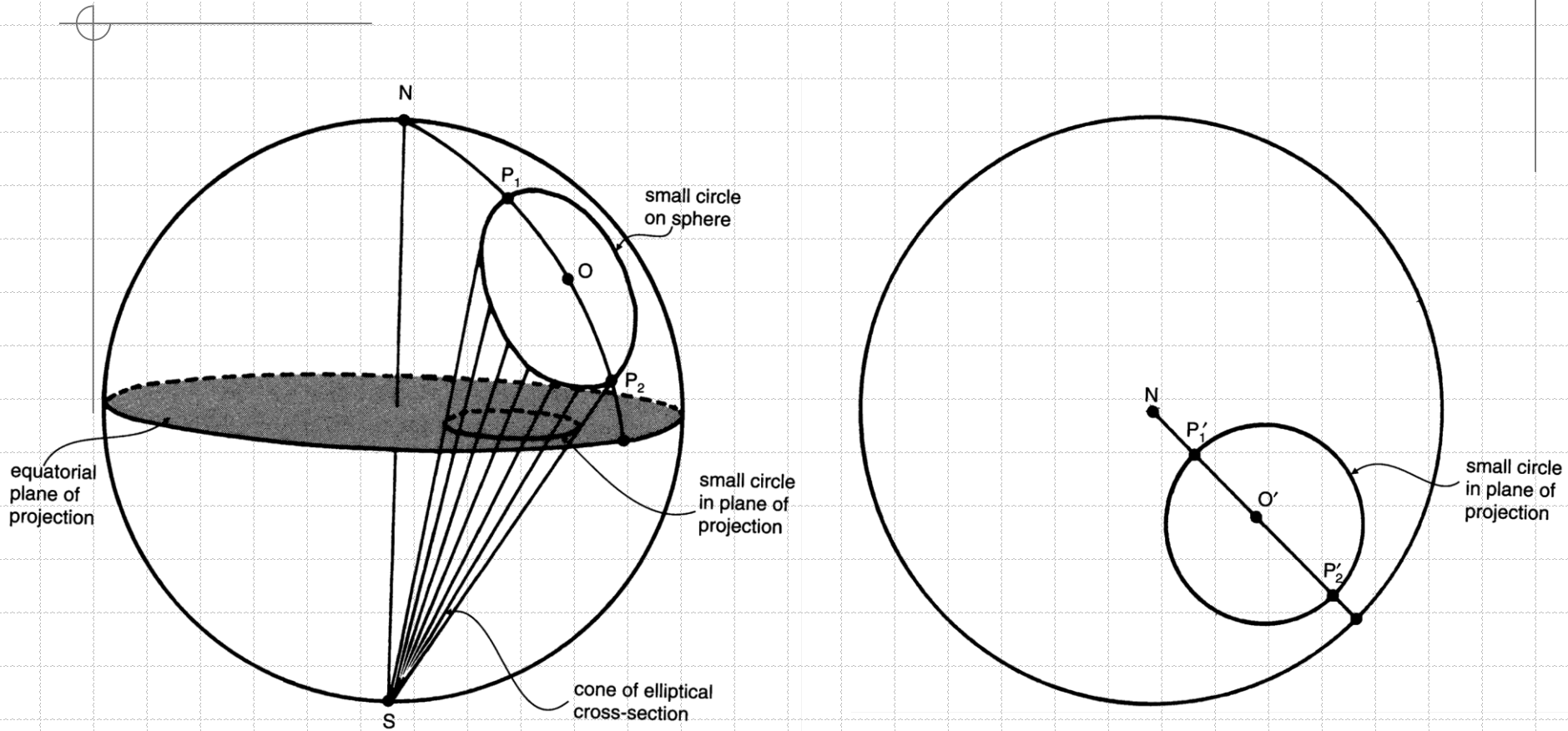
# The Stereographic Projection



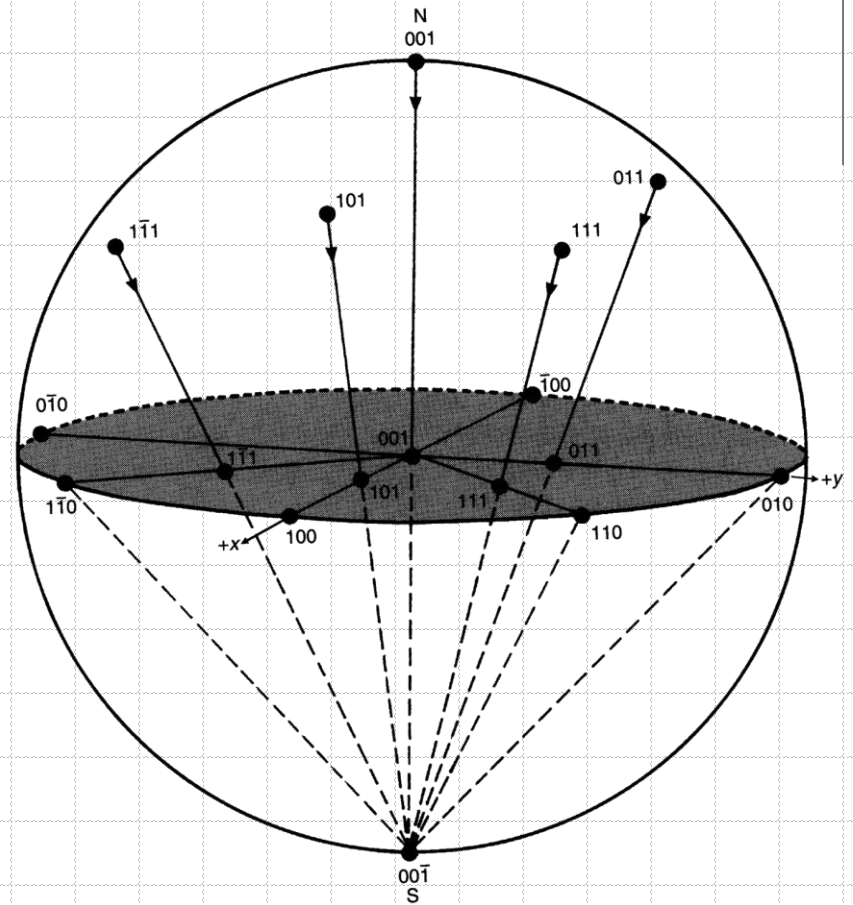
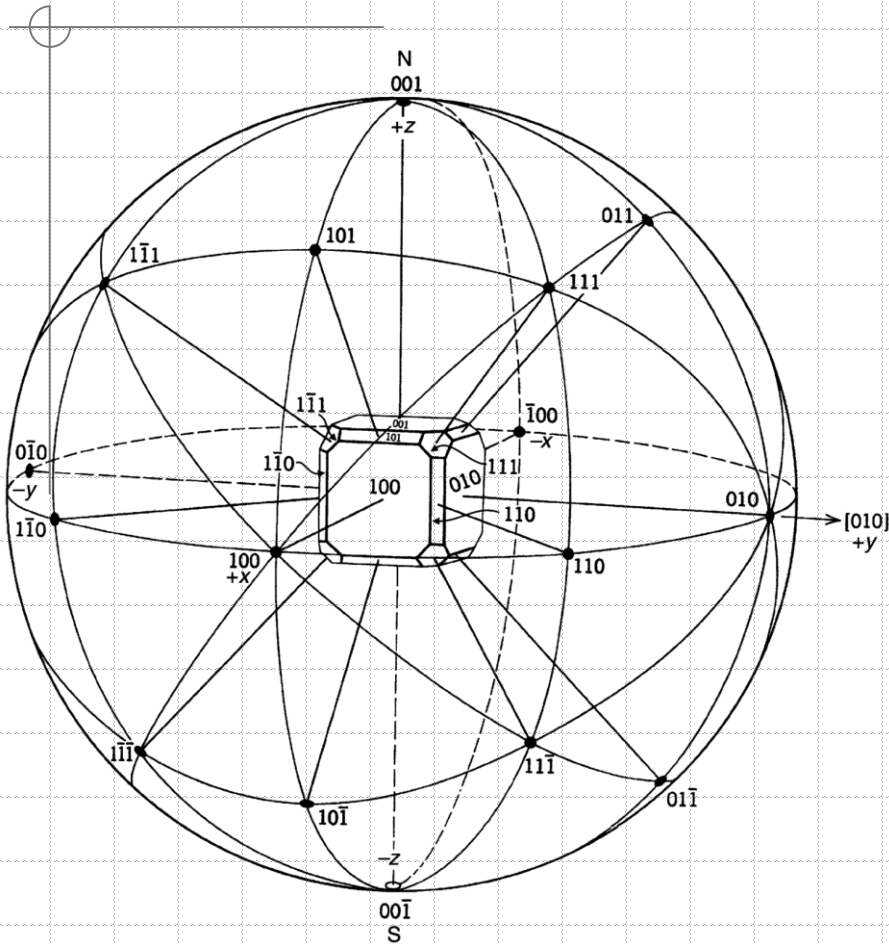
As we look down to the earth

The stereographic projection

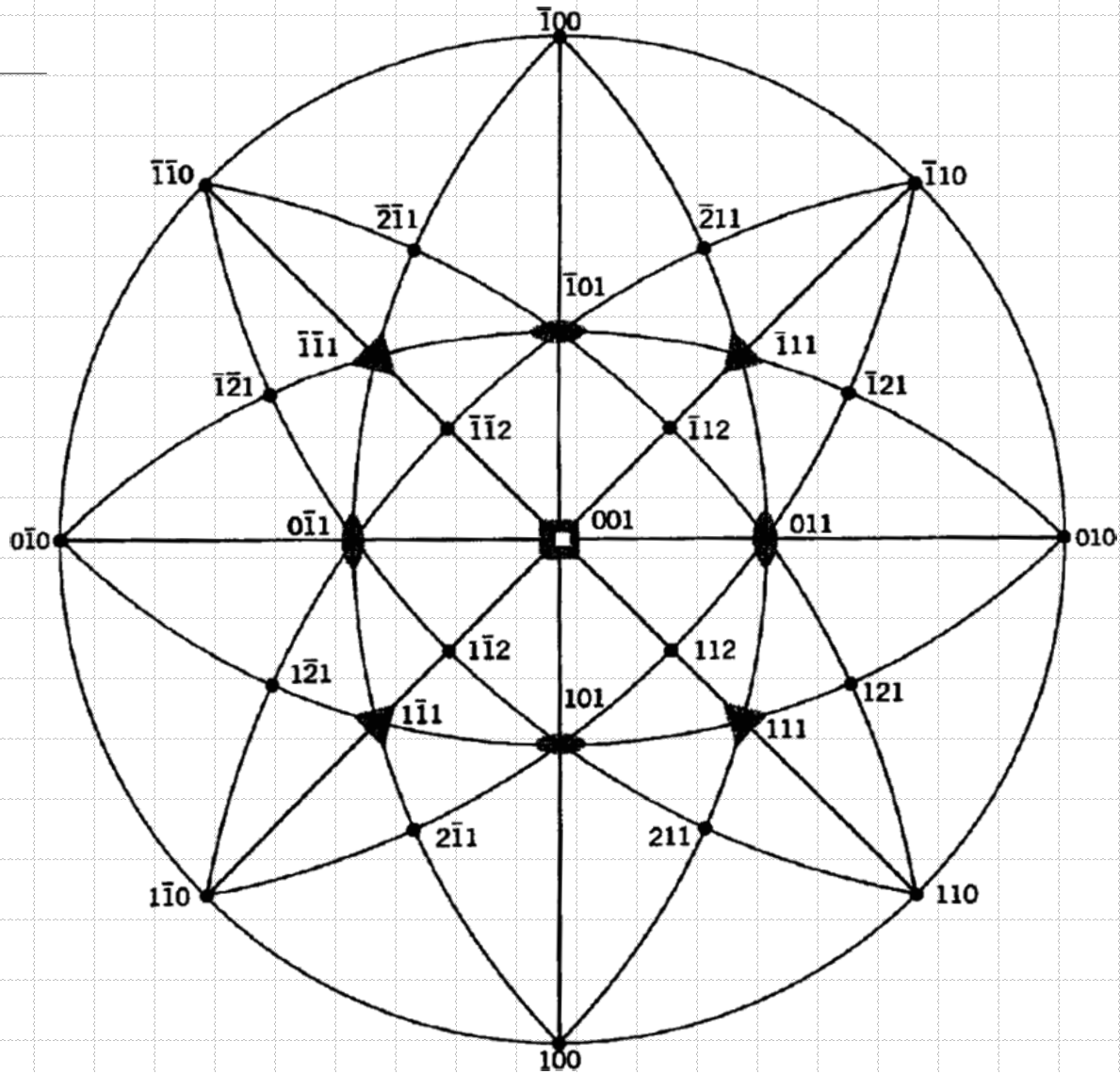
# The Stereographic Projection



# The Pole Figures



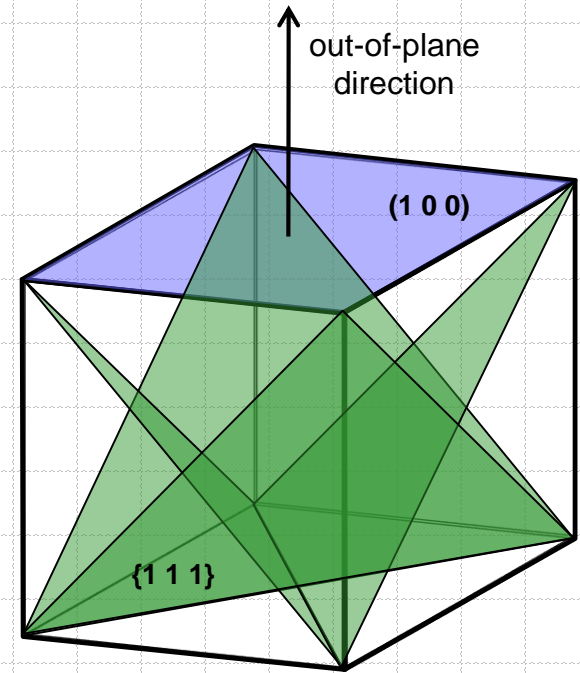
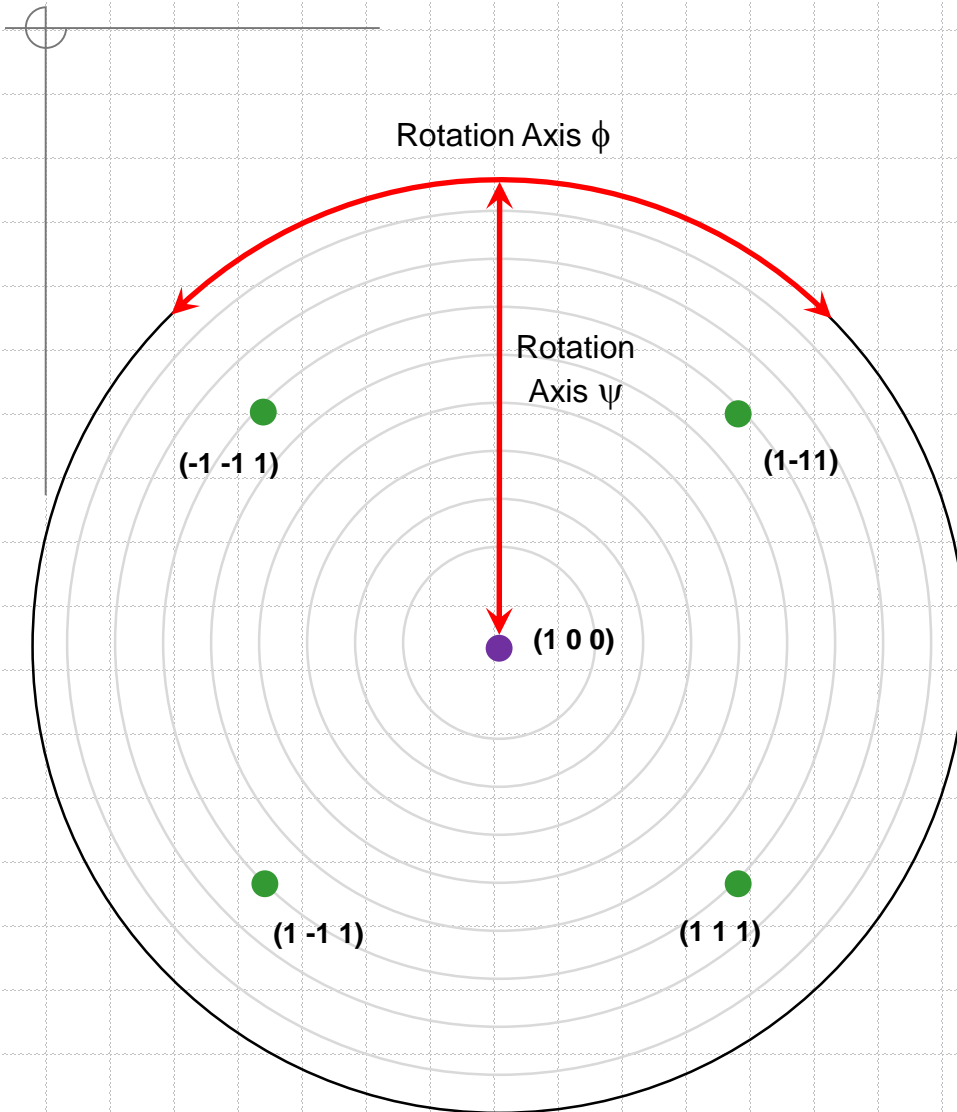
# The Pole Figures



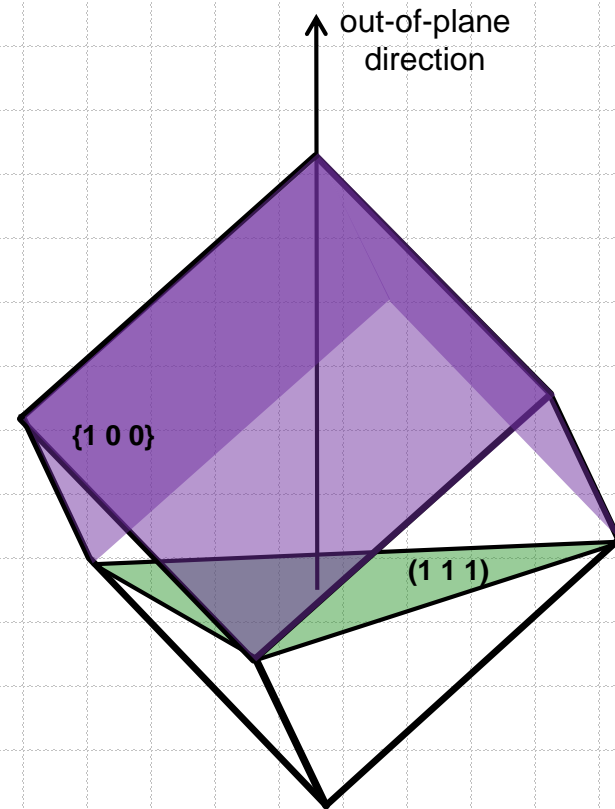
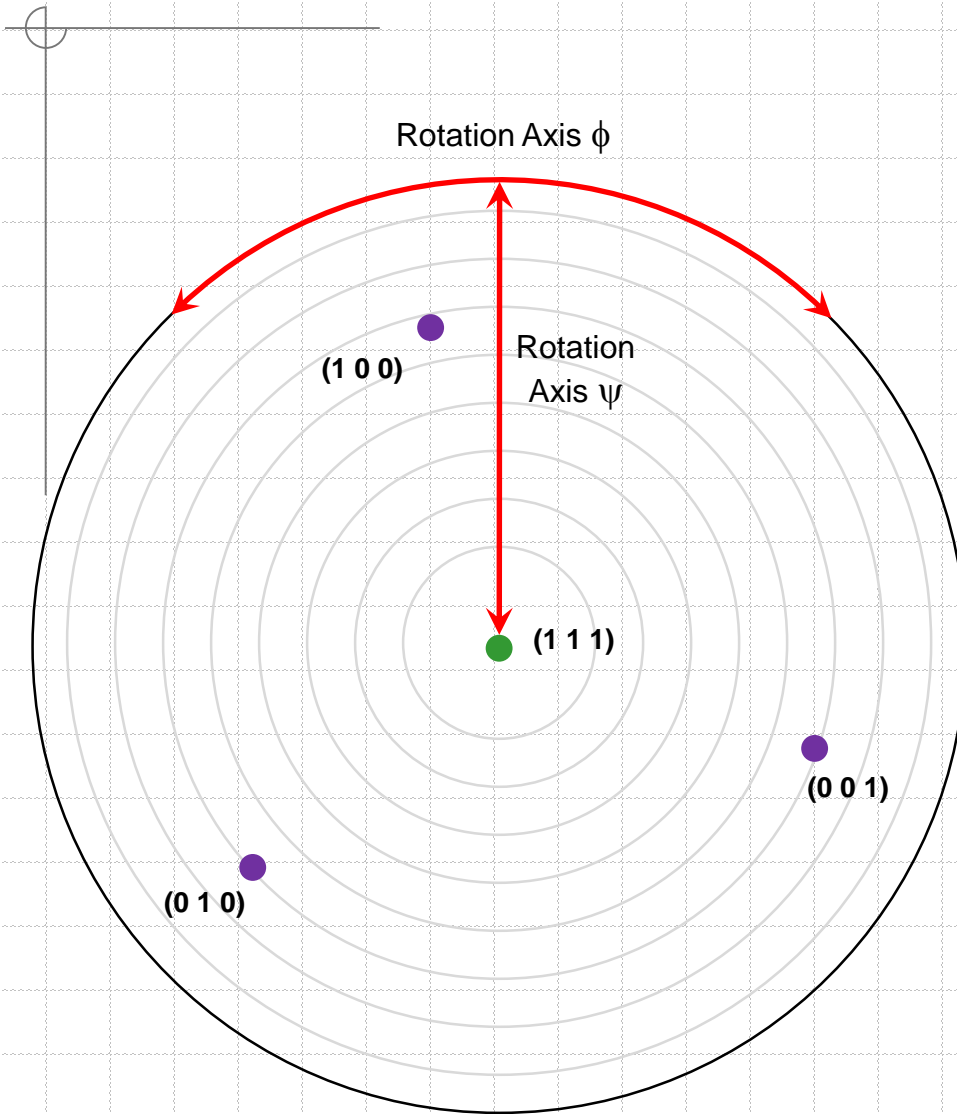
# The Pole Figures

- ◆ We now project the sphere with its pole density onto a plane. This projection is called a pole figure.
  - A pole figure is scanned by measuring the diffraction intensity of a given reflection with constant  $2\theta$  at a large number of different angular orientations of a sample.
  - A contour map of the intensity is then plotted as a function of the angular orientation of the specimen.
  - The intensity of a given reflection is proportional to the number of hkl planes in reflecting condition.
  - Hence, the pole figure gives the probability of finding a given (h k l) plane normal as a function of the specimen orientation.
  - If the crystallites in the sample have random orientation the contour map will have uniform intensity contours.

# The Pole Figures

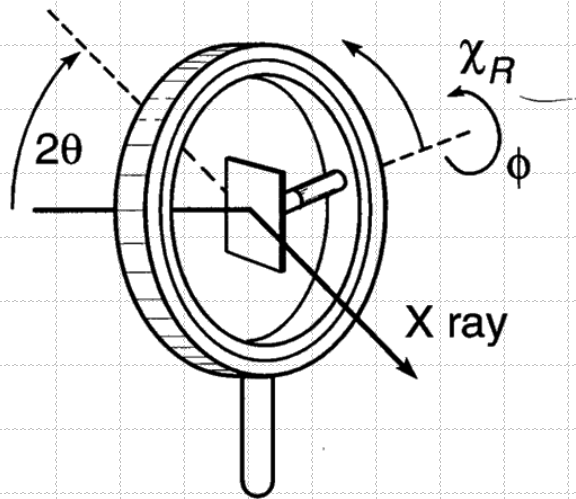


# The Pole Figures

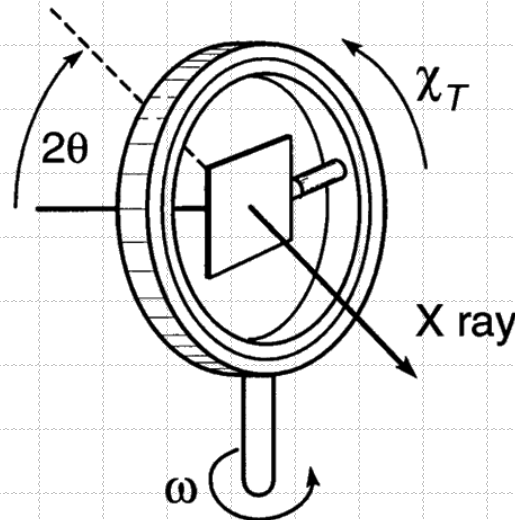


# Texture Measurements

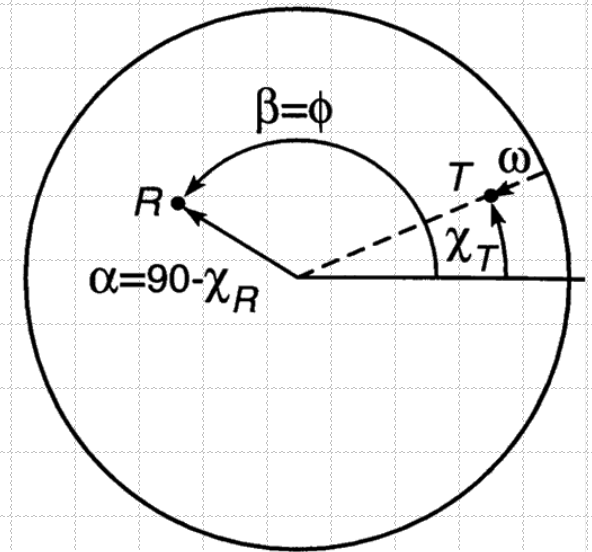
- ◆ Requires special sample holder which allows rotation of the specimen in its own plane about an axis normal to its surface,  $\phi$ , and about a horizontal axis,  $\chi$ .



Reflection

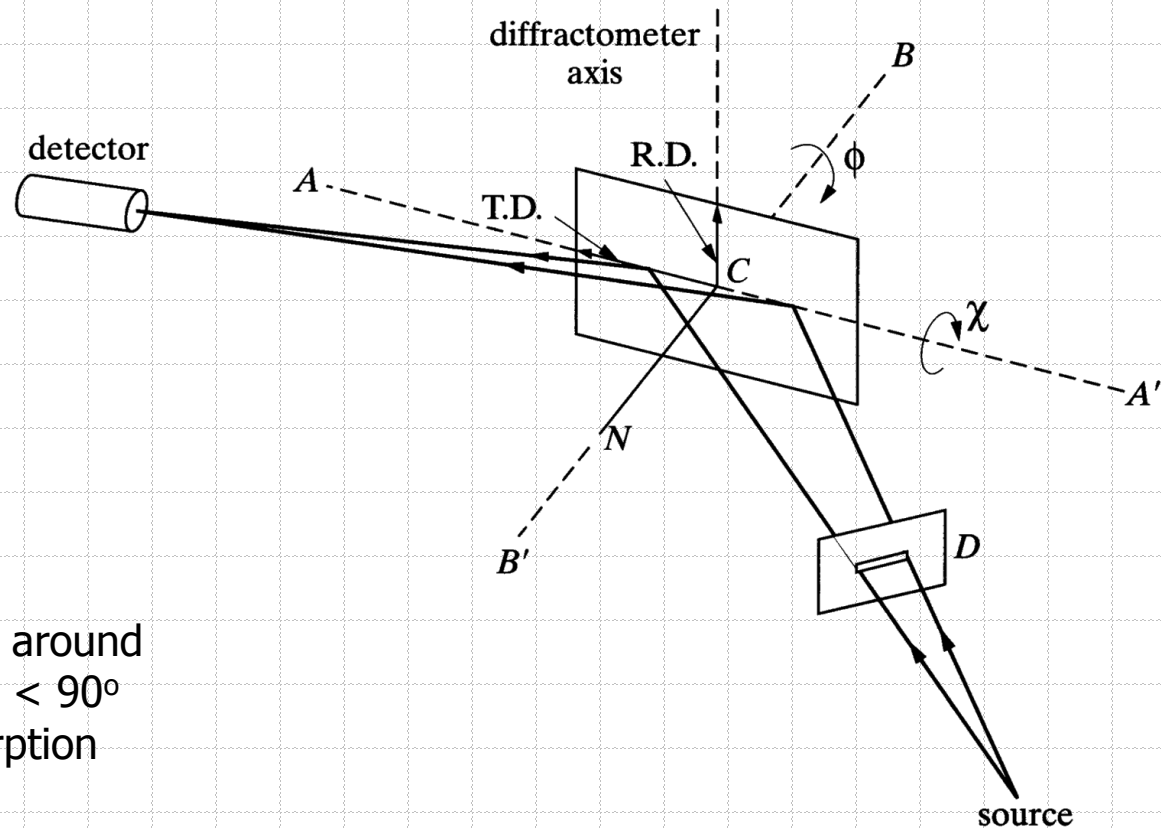


Transmission



# Schulz Reflection Method

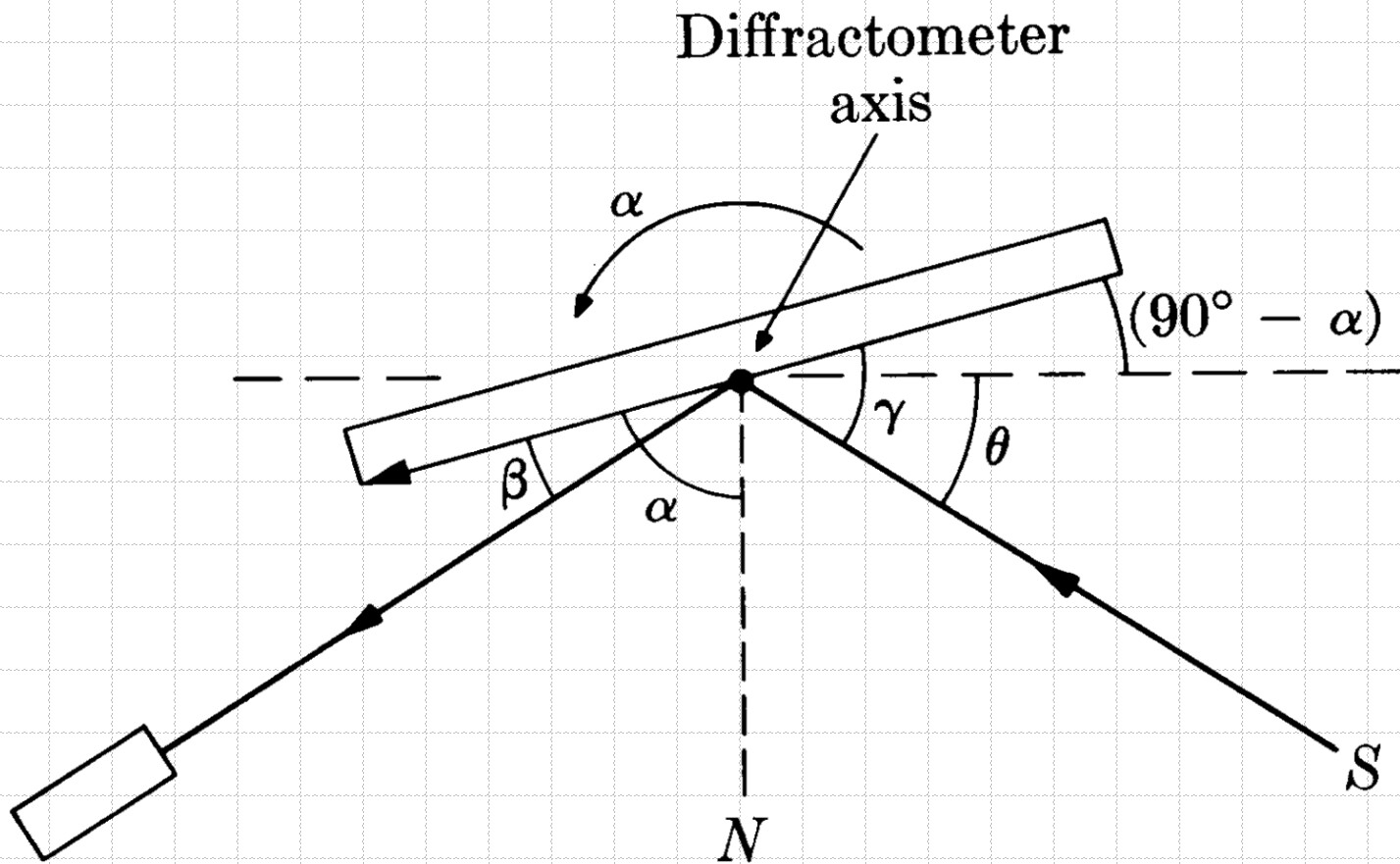
- ◆ In the Bragg-Brentano geometry a divergent x-ray beam is focused on the detector.
- ◆ This no longer applies when the sample is tilted about  $\chi$ .



Advantage: rotation in around  $\chi$  in the range  $40^\circ < \chi < 90^\circ$  does not require absorption correction.

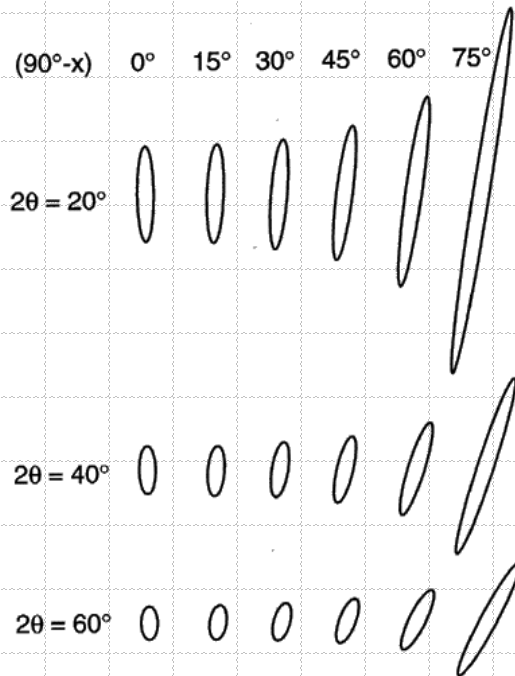
# Field and Merchant Reflection Method

- ◆ The method is designed for a parallel incident beam.

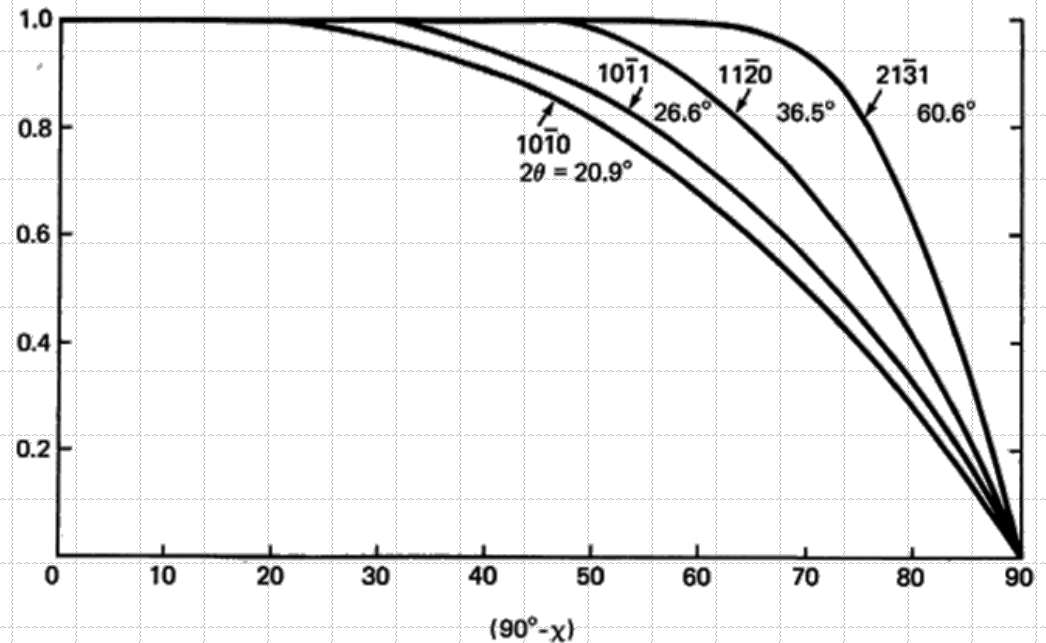


# Defocusing Correction

- ◆ As sample is tilted in  $\chi$ , the beam spreads out on a surface.
- ◆ At high  $\chi$  values not all the beam enters the detector.
- ◆ Need for defocusing correction.



Change in shape and orientation of the irradiated spot on a sample surface for different sample inclinations as a function of tilt angle  $\alpha$  and Bragg angle  $2\theta$ . The incident beam is cylindrical.



Intensity correction for x-ray pole figure determination in reflection geometry. Selected reflections for quartz.

# Absorption Correction

- ◆ Diffracted intensities must be corrected for change in absorption due to change in  $\alpha$ .

$$dI_D = \frac{I_0 ab}{\sin \gamma} e^{-\mu x(1/\sin \gamma + 1/\sin \beta)} dx$$

$a$  – volume fraction of a specimen containing particles having correct orientation for reflection of the incident beam.

$b$  – fraction of the incident energy which is diffracted by unit volume

substitute

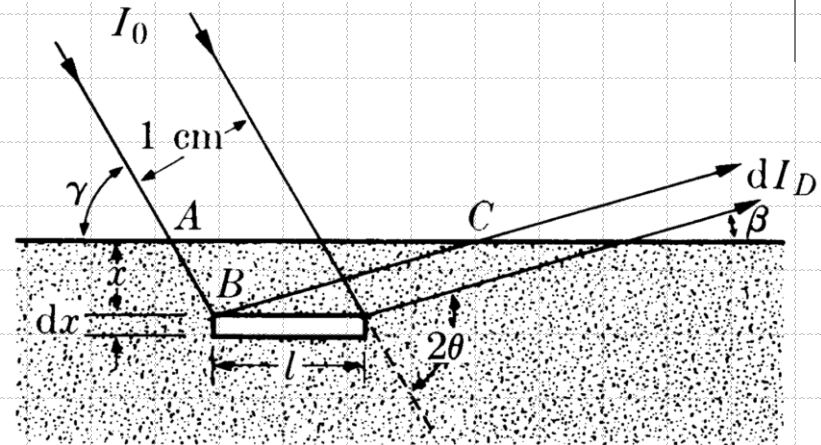
$$\gamma = \theta + (90^\circ - \alpha), \quad \beta = \theta - (90^\circ - \alpha)$$

Integrate  $0 < x < \infty$

$$I_D = \frac{I_0 ab}{\mu \{1 - [\cos(\alpha - \theta) / \cos(\alpha + \theta)]\}}$$

We interested in the intensity at angle  $\alpha$ , relative to intensity at  $\alpha = 90^\circ$ :

$$S = \frac{I_D(\alpha = \alpha)}{I_D(\alpha = 90^\circ)} = 1 - \cot \alpha \cot \theta$$



# Pole Figure Measurement

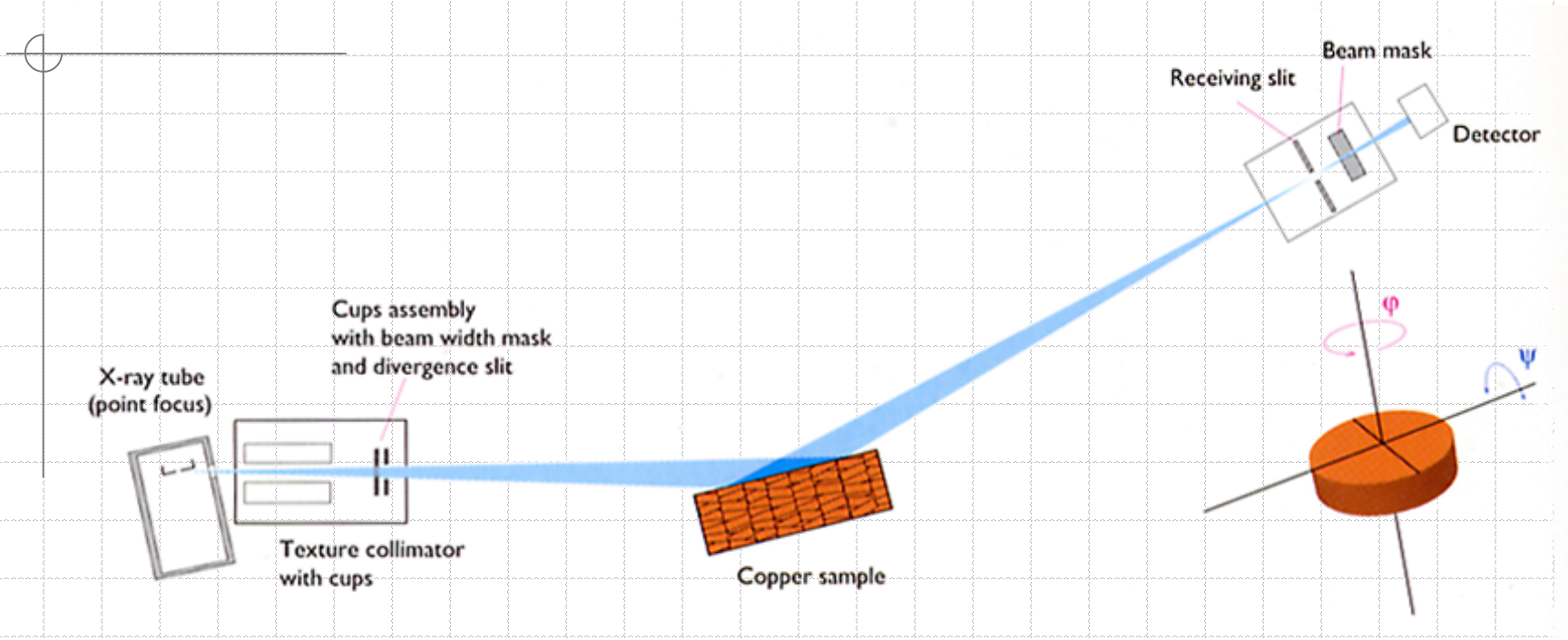
- ◆ Pole figure diffractometer consists of a four-axis single-crystal diffractometer.

Rotation axes:

$\theta$ ,  $\omega$ ,  $\chi$ , and  $\phi$

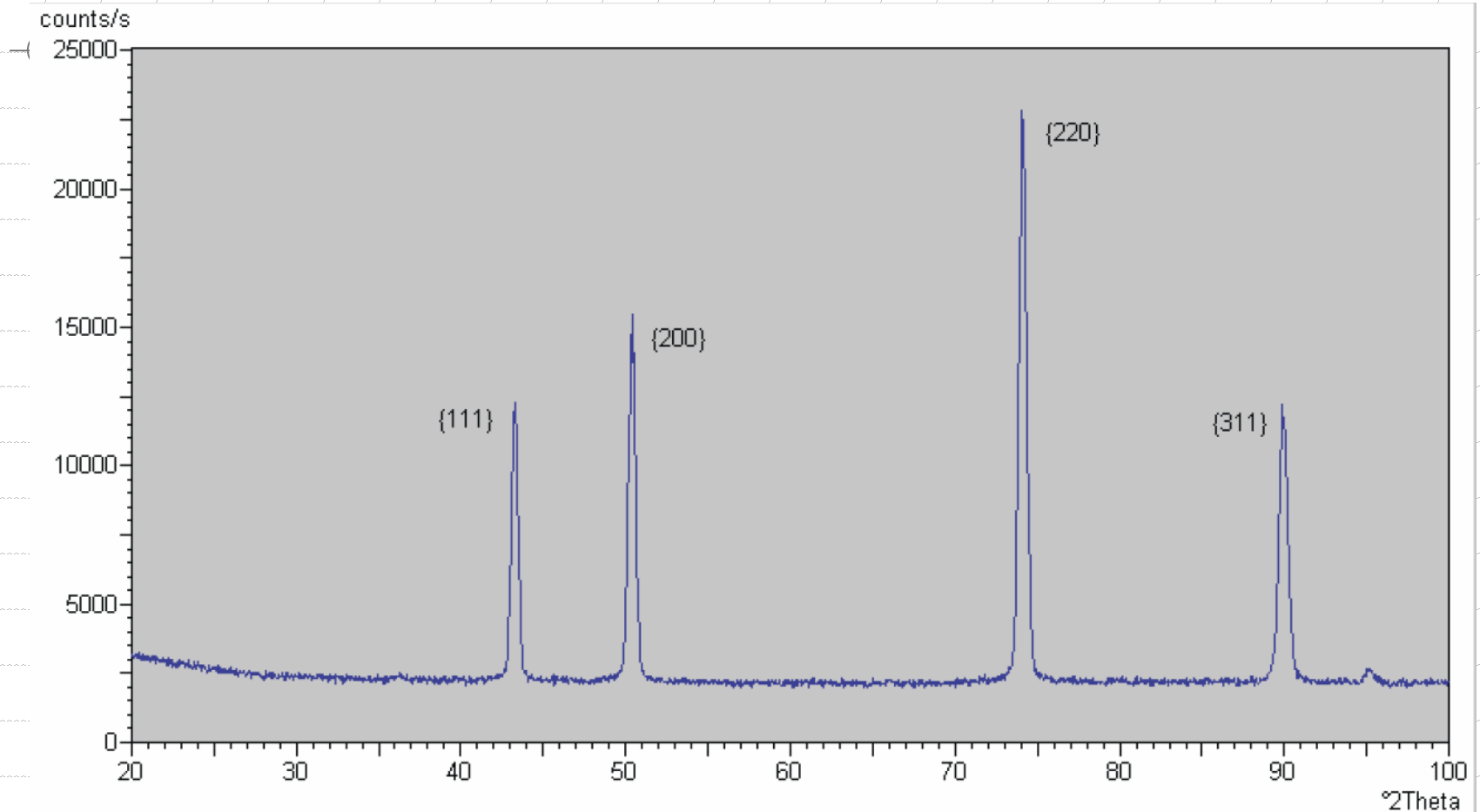


# Example: Rolled Copper



- Texture measurements were performed on Cu disk  $\varnothing = 22$  mm,  $t = 0.8$  mm.
- Four pole figures (111), (200), (220) and (311) were collected using Schulz reflection method.
- Background intensities were measured next to diffraction peaks with offset  $2\theta = \pm 4^\circ$ .
- Defocusing effects were corrected using two methods:
  - measured texture free sample
  - calculated (FWHM of the peaks at  $\psi = 0^\circ$  is required – obtained from  $\theta$ - $2\theta$  scan).
- X'Pert Texture program was used for quantitative analysis.

# Example: Rolled Copper



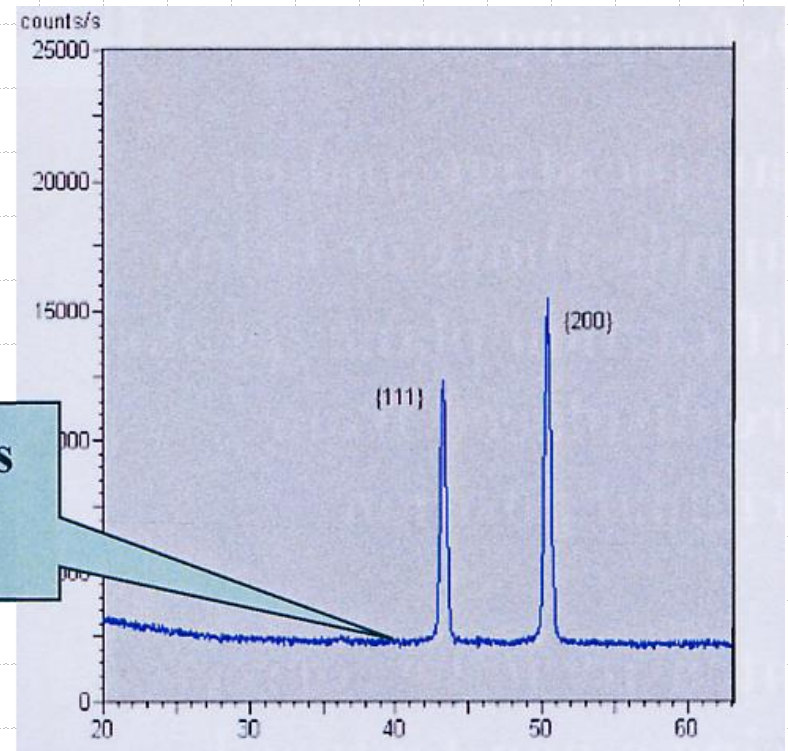
- Measure  $\theta$ - $2\theta$  scan in order to determine the reflections used for the pole figure measurements.
- Use FWHM of the peaks to calculate the defocusing curve.

# Example: Rolled Copper

## Background Correction

- Pole figure intensities include background.
- Correction for background radiation is performed by measuring the intensity vs.  $\psi$ -tilt next to the diffraction peak.

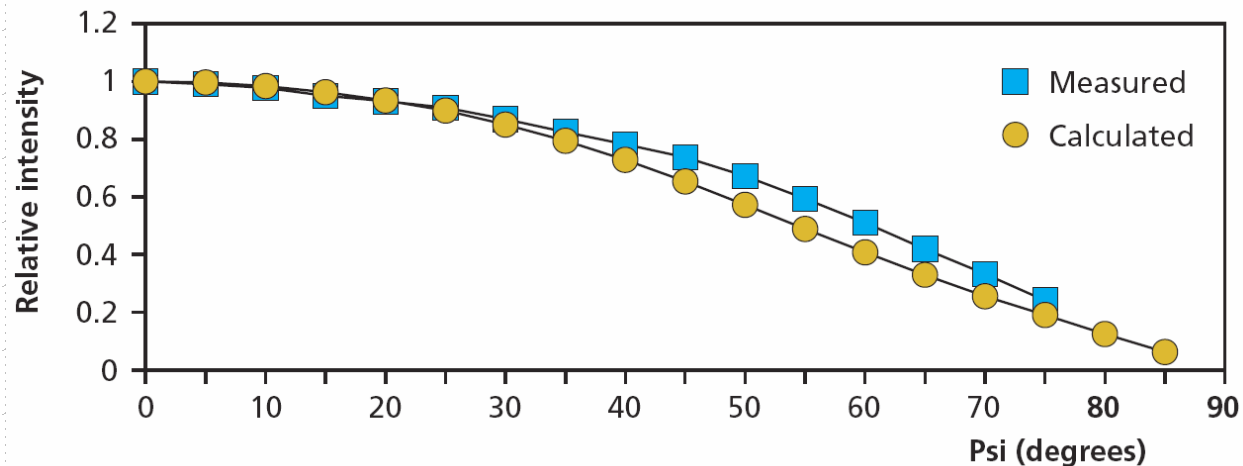
**Background correction measurements beside the peaks**



# Example: Rolled Copper

## Corrections

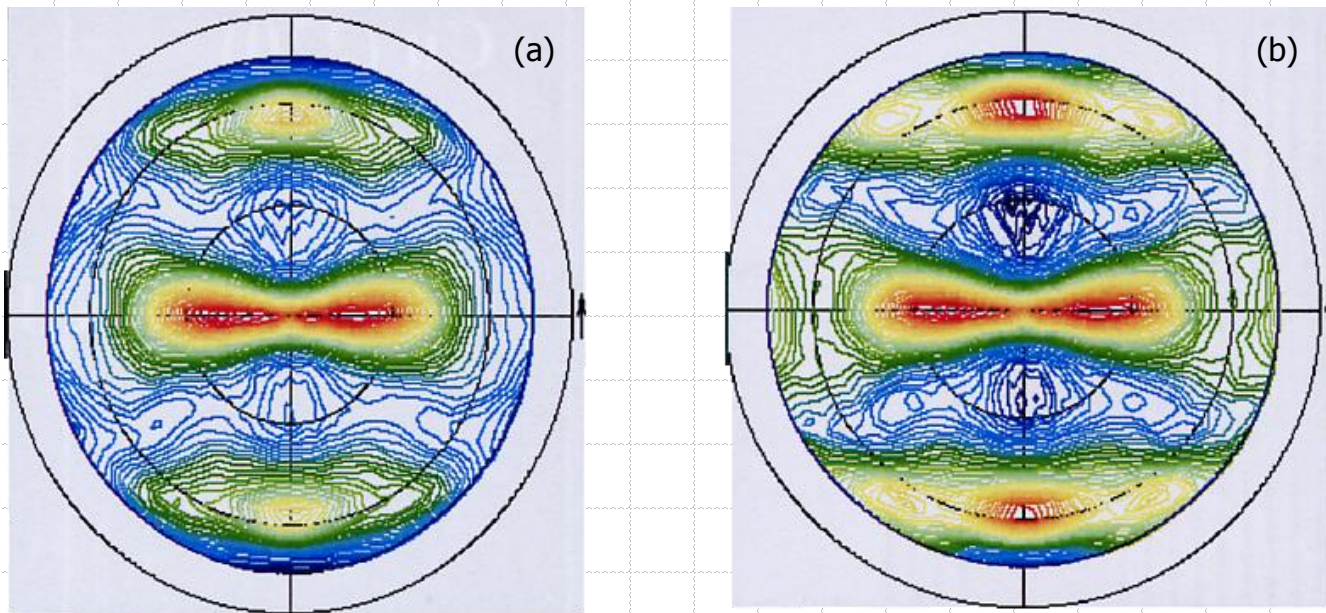
- Experimental pole figures are corrected for background intensities.
- Either experimental or theoretical defocusing correction curve is applied.



Measured and calculated defocusing corrections for Cu(220) pole figure

# Example: Rolled Copper

## Corrections

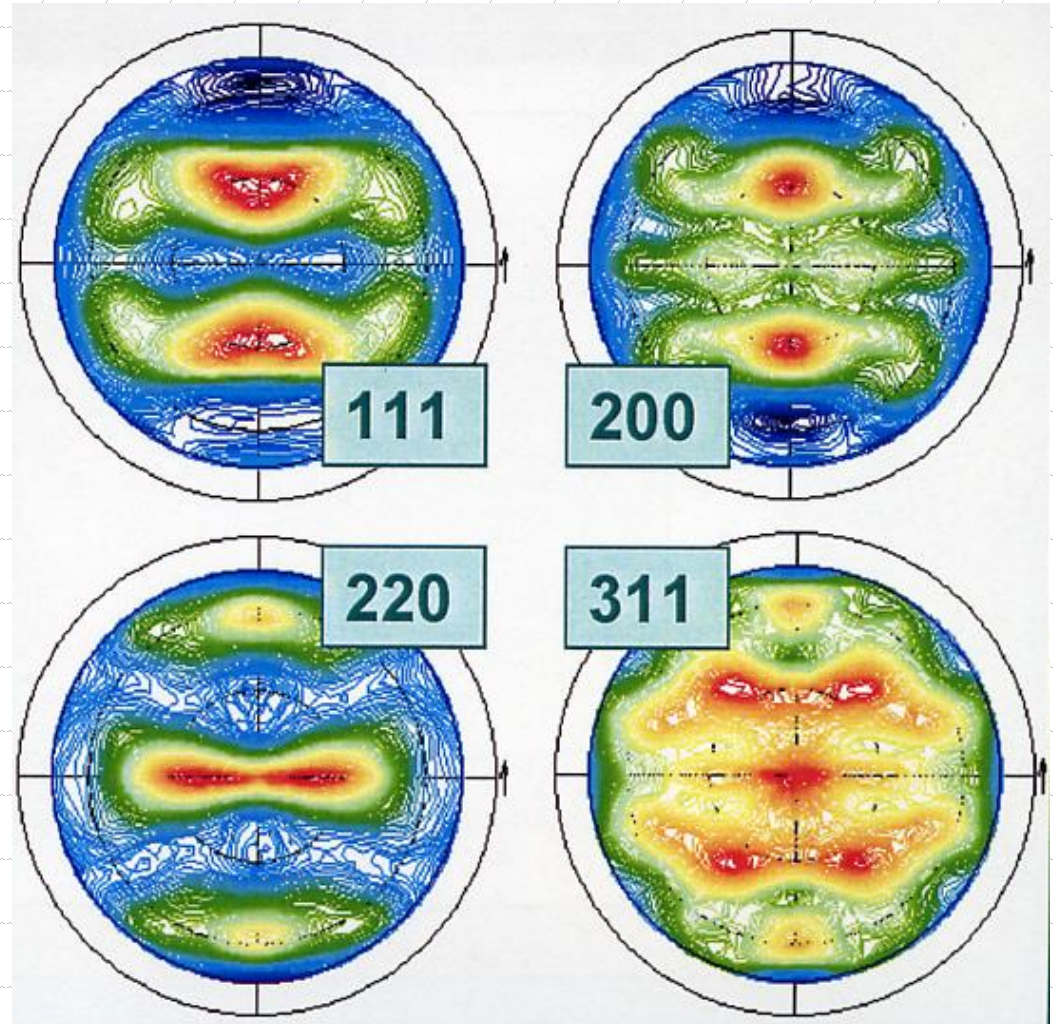


- 2D representation of Cu(220) pole figure as (a) measured and (b) corrected.
- The most noticeable effect is at higher  $\psi$ -tilt angles.

# Example: Rolled Copper

## Pole Figure Measurements

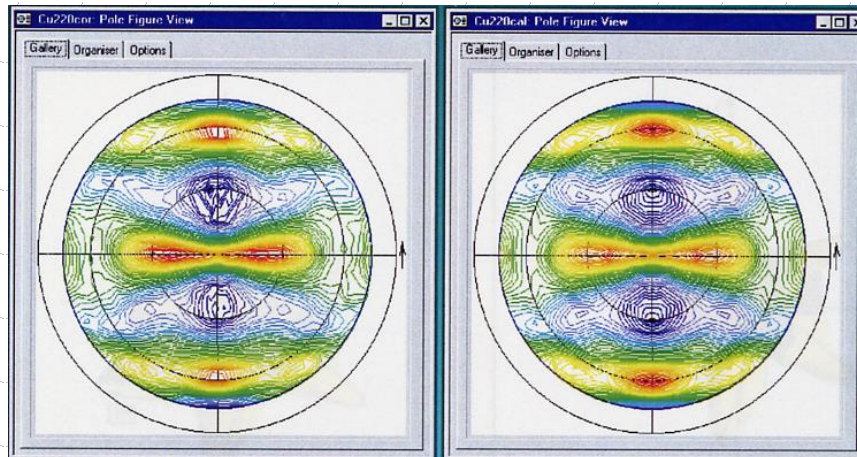
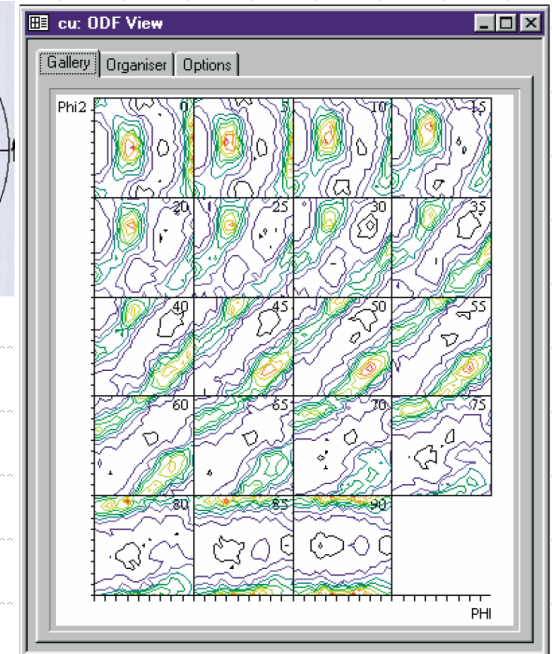
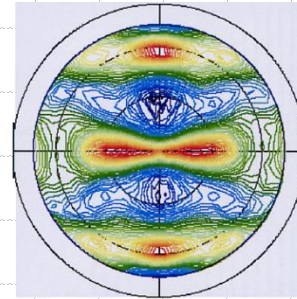
- Four pole figures have been measured.
- Symmetry of rolling process is obtained from the pole figures:
  - pole figure is symmetrical around  $\phi = 0^\circ$  and  $\phi = 90^\circ$ .
- The symmetry is called orthorhombic sample symmetry.



# Example: Rolled Copper

## Orientation Distribution Function Calculation

- X'Pert Texture calculates ODF
- When ODF is available X'Pert Texture can calculate pole figures and inverse pole figures for any set of (hkl).

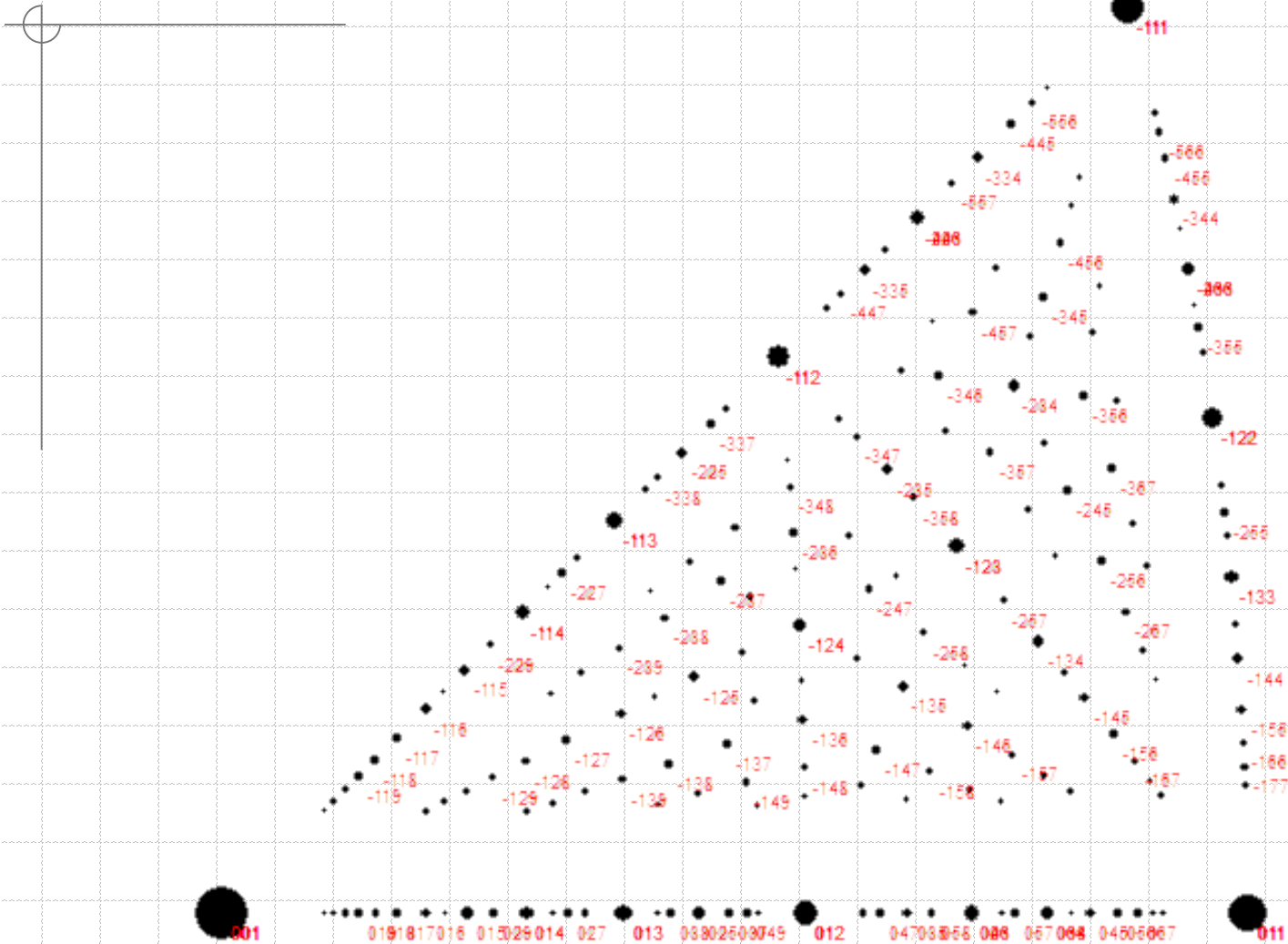


Measured

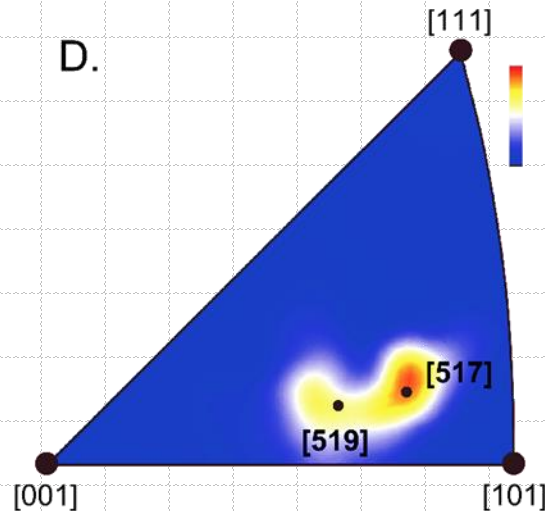
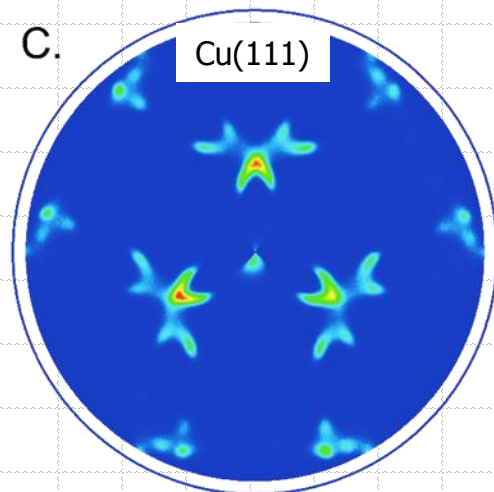
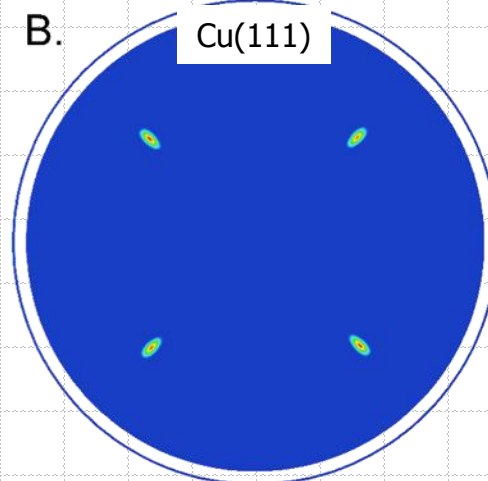
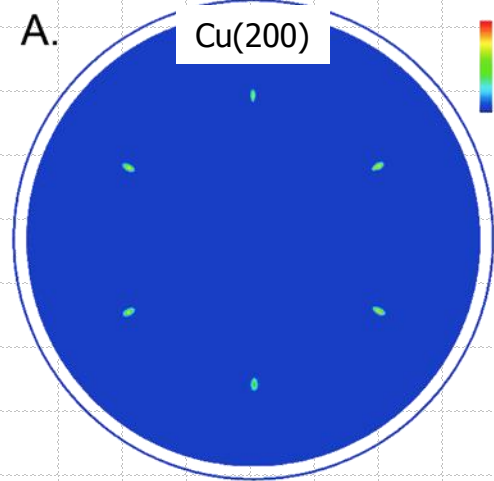
Calculated



# Inverse Pole Figures

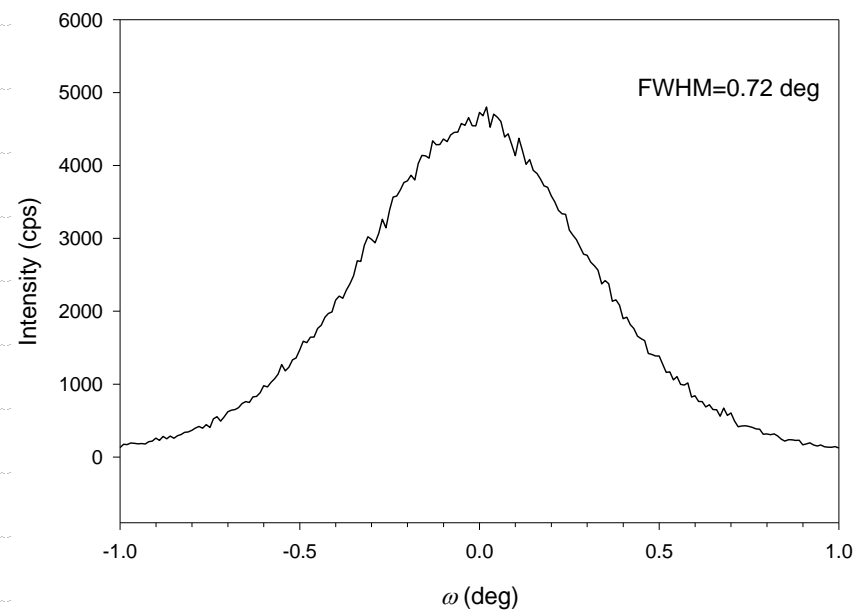
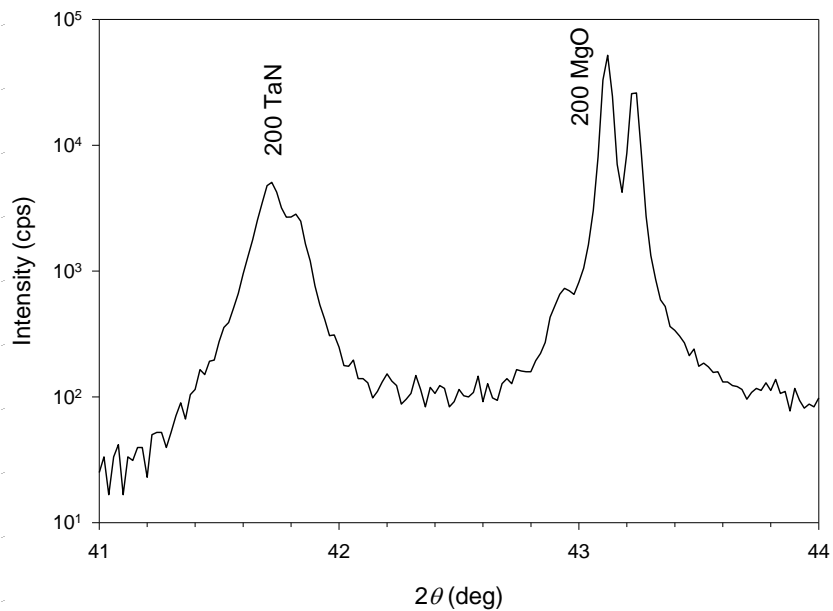
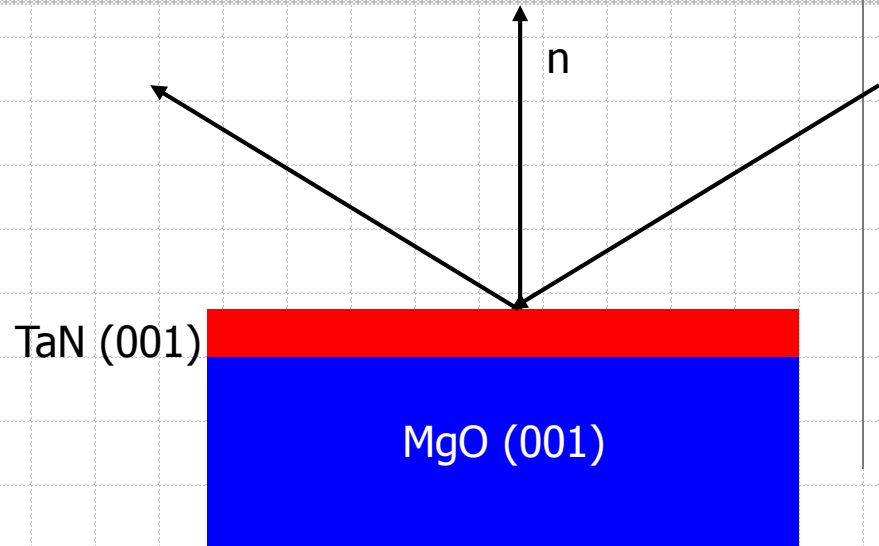
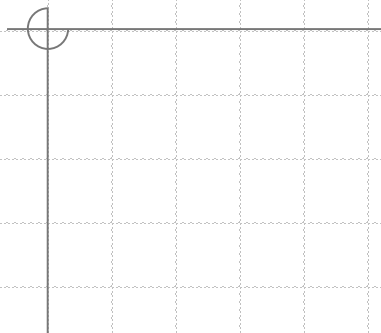


# Engineering Cu surfaces for the electrocatalytic conversion of CO<sub>2</sub>



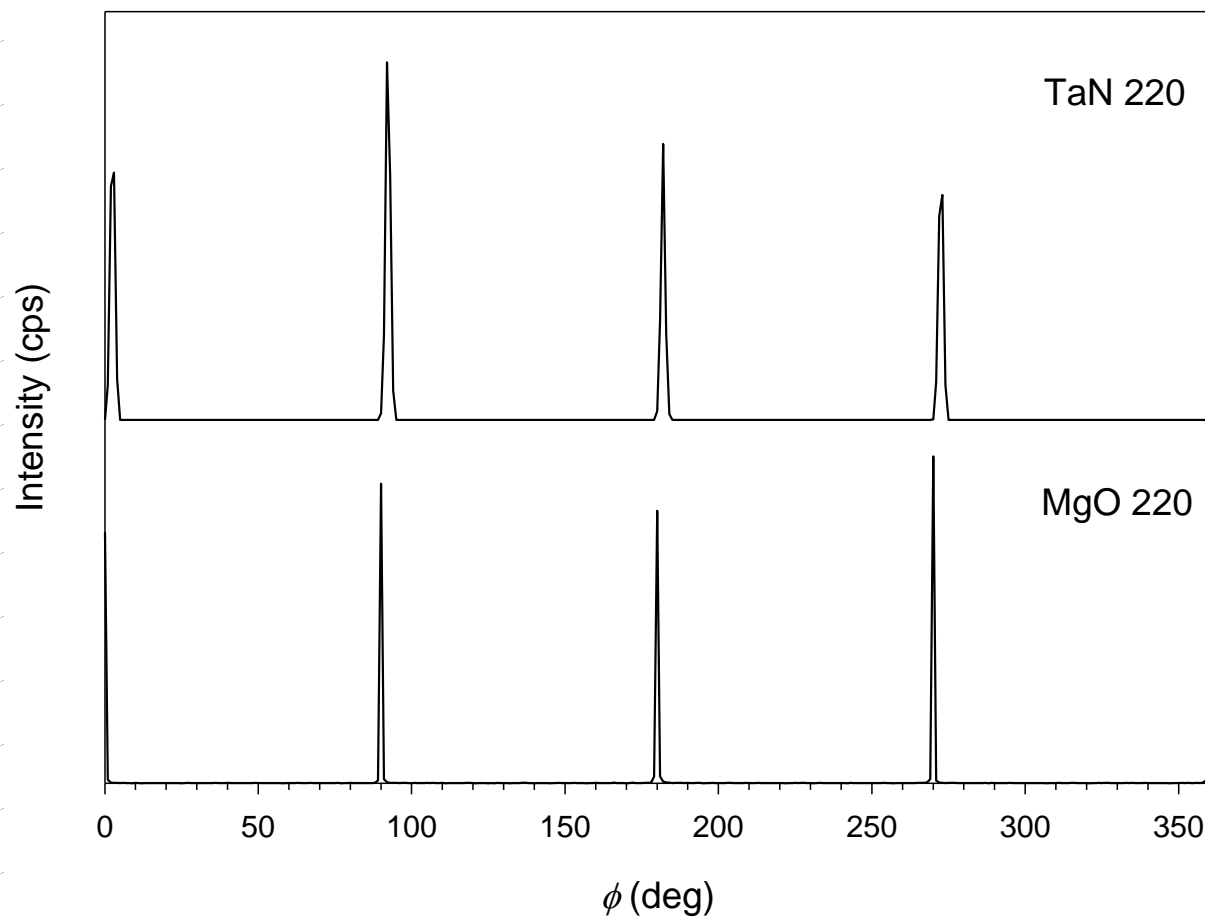
- X-ray pole figures for:
- (A) Cu on Al<sub>2</sub>O<sub>3</sub>(0001); Cu(200) intensities are shown.
  - (B) Cu on Si(100); Cu(111) intensities are shown.
  - (C) Cu on Si(111); Cu(111) intensities are shown.
  - (D) Inverse pole figure shows highest intensities for the (751) plane, indicating that Cu on Si(111) is predominantly oriented in the [517] direction out-of-plane.

# TaN Thin Film



# TaN Thin Film

◆  $\phi$ -scan of TaN (202) and MgO (202) reflections.



# TaN Thin Film

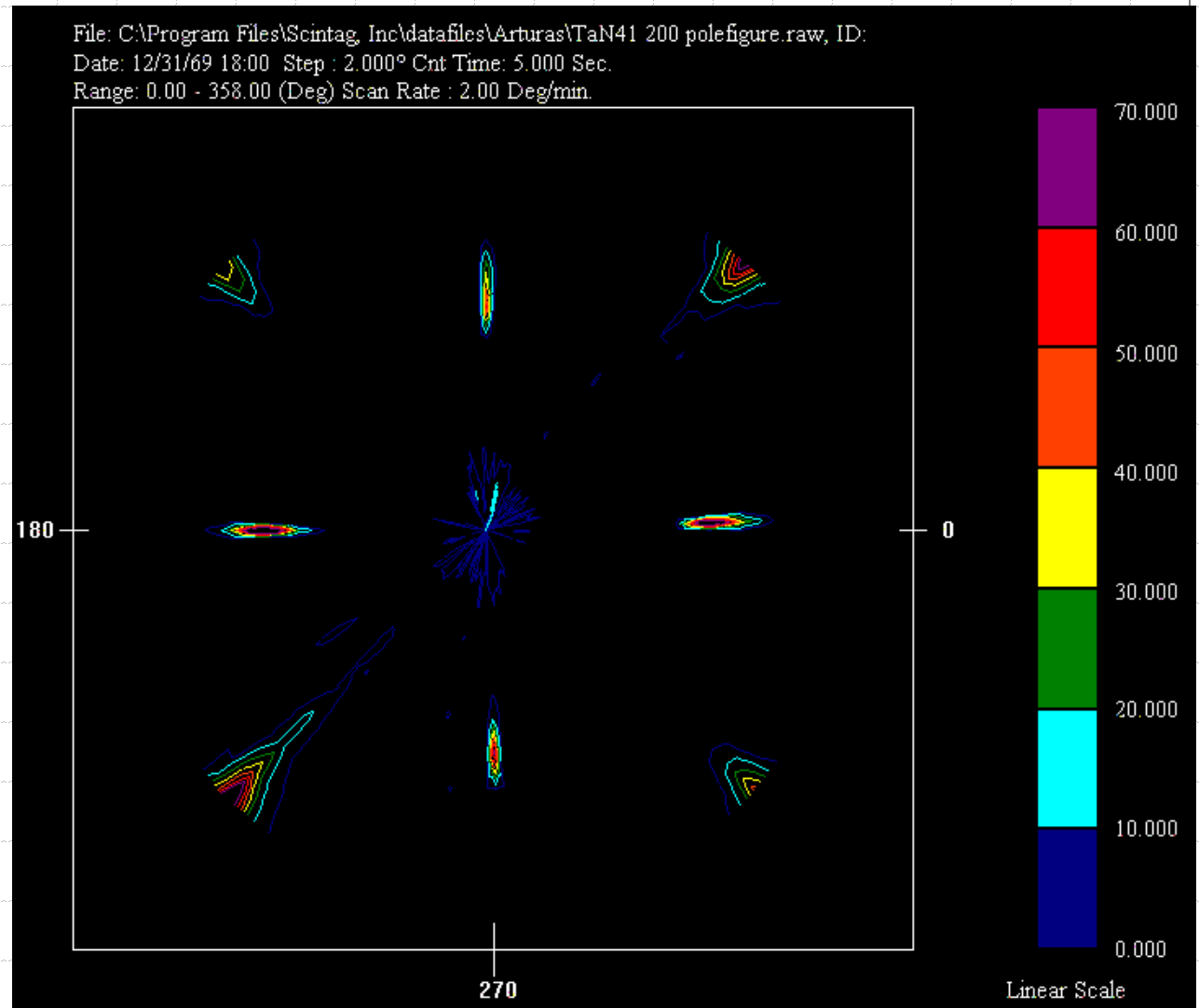
- ◆ TEM reveals additional structure.

TaN23

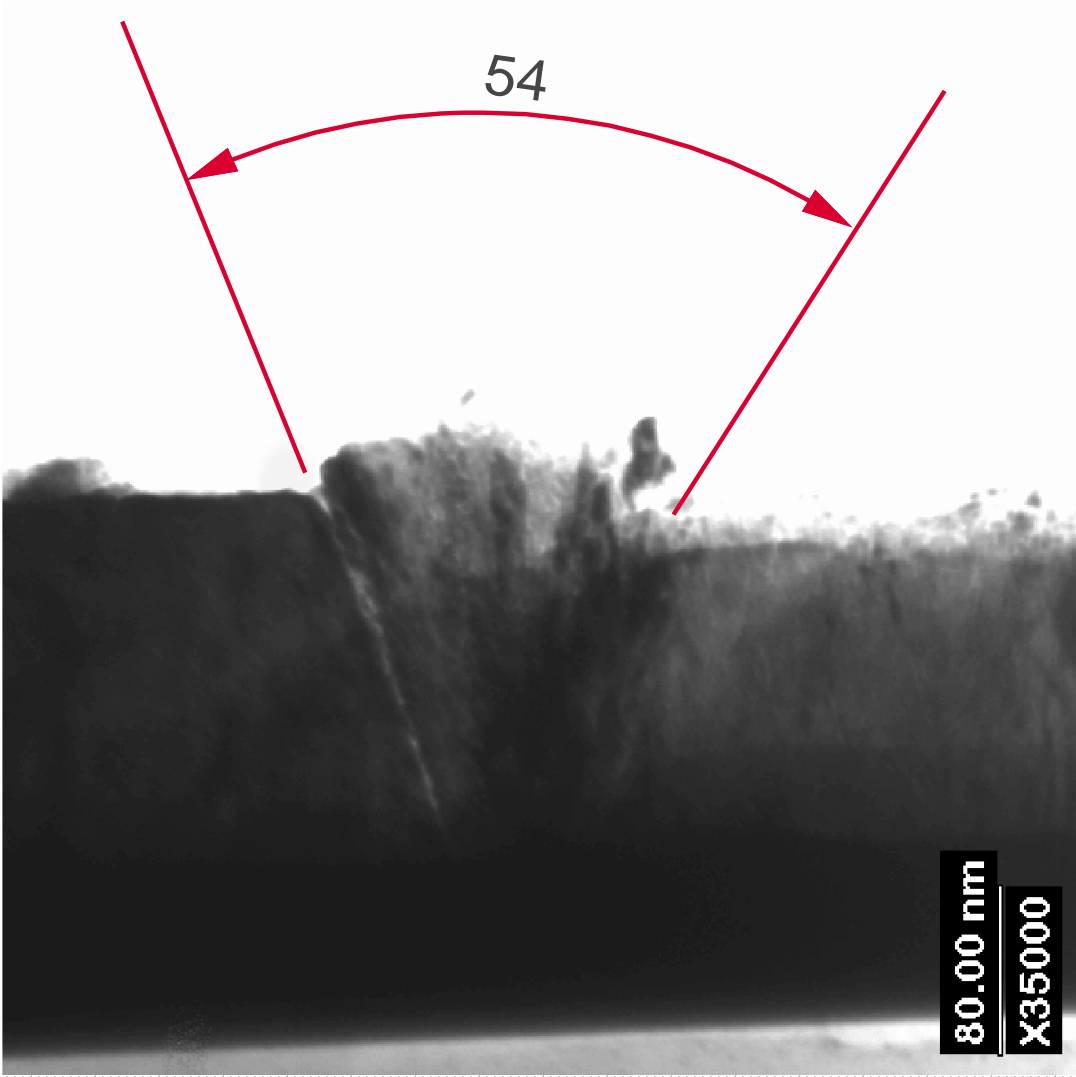
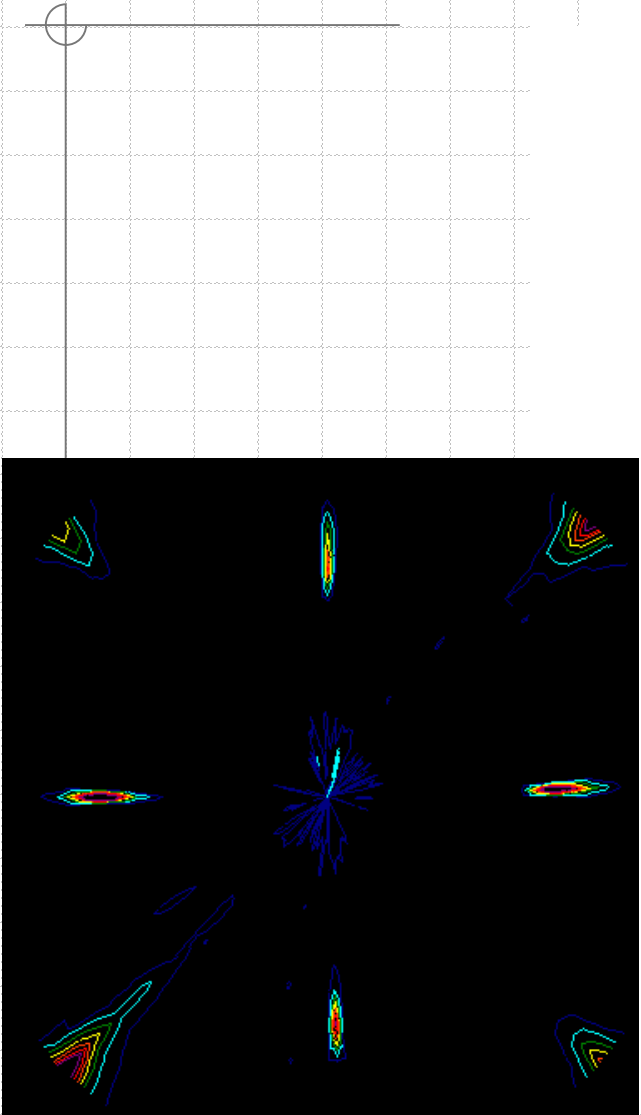


# TaN Thin Film

◆ XRD 002 pole figure of TaN film

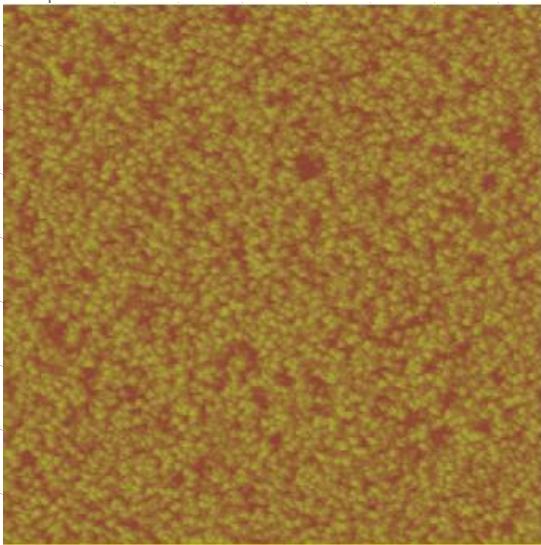


# TaN Thin Film

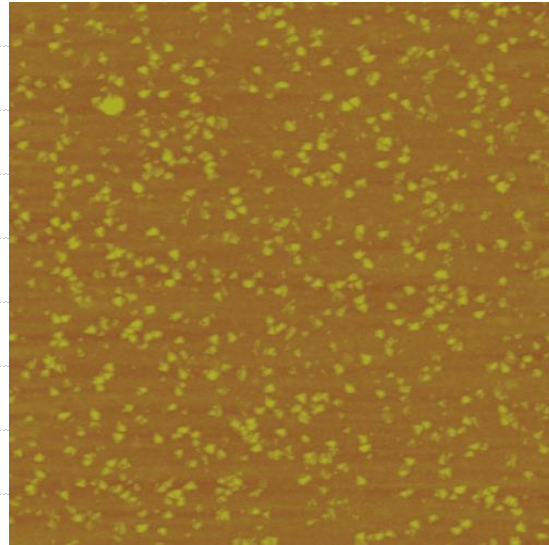


# TaN Thin Film

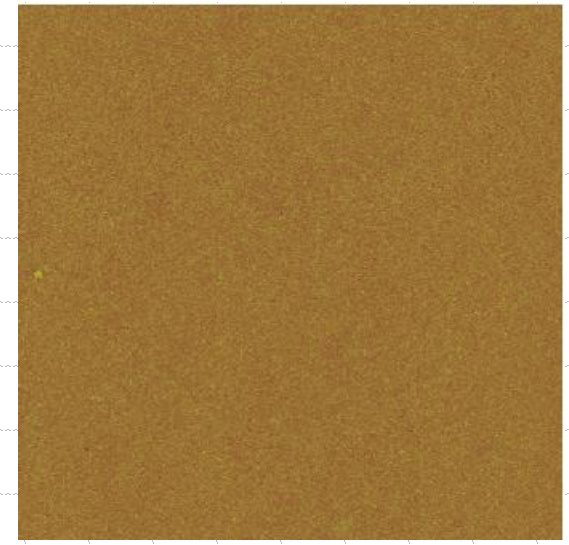
- ◆ Atomic Force Microscopy images of TaN films prepared under different  $N_2$  partial pressure



$p_N=2$  mTorr



$p_N=2.5$  mTorr



$p_N=4$  mTorr